Inorganic Chemistry

Forum Article

pubs.acs.org/IC

Hydricity of an Fe–H Species and Catalytic CO_2 Hydrogenation

Henry Fong and Jonas C. Peters*

Division of Chemistry and Chemical Engineering, California Institute of Technology, Pasadena, California 91125, United States

Supporting Information

ABSTRACT: Despite renewed interest in carbon dioxide (CO_2) reduction chemistry, examples of homogeneous iron catalysts that hydrogenate CO_2 are limited compared to their noble-metal counterparts. Knowledge of the thermodynamic properties of iron hydride complexes, including M–H hydricities (ΔG_{H^-}), could aid in the development of new iron-based catalysts. Here we present the experimentally determined hydricity of an iron hydride complex: $(SiP^{iPr}_3)Fe(H_2)(H)$, ΔG_{H^-} = 54.3 ± 0.9 kcal/mol [SiP^{iPr}_3 = $[Si(o\text{-}C_6H_4PiPr_2)_3]^-$]. We also explore the CO_2 hydrogenation chemistry of a series of triphosphinoiron complexes, each with a distinct apical unit on the ligand chelate (Si^-, C^-, PhB^-, N, B). The silyliron $(SiP^R_3)Fe$ (R = *i*Pr and Ph) and boratoiron $(PhBP^{iPr}_3)Fe$ ($PhBP^{iPr}_3$ = $[PhB(CH_2PiPr_2)_3]^-$) systems, as well as the recently reported $(CP^{iPr}_3)Fe$ (CP^{iPr}_3 = $[C(o\text{-}C_6H_4PiPr_2)_3]^-$), are also catalysts for CO_2 hydrogenation in methanol and in the presence of triethylamine, generating methylformate and triethylammonium formate at up to 200 TON using $(SiP^{Ph}_3)FeCl$ as the precatalyst. Under stoichiometric conditions, the iron hydride complexes of this series react with CO_2 to give formate complexes. Finally, the proposed mechanism of the (SiP^{iPr}_3)-Fe system proceeds through a monohydride intermediate $(SiP^{iPr}_3)Fe(H_2)(H)$, in contrast to that of the known and highly active tetraphosphinoiron, (tetraphos)Fe (tetraphos = $P(o\text{-}C_6H_4PPh_2)_3$), CO_2 hydrogenation catalyst.

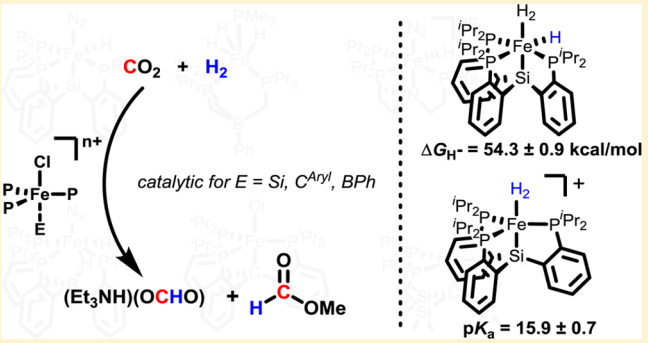

INTRODUCTION

The reduction of carbon dioxide (CO_2) into value-added chemicals and liquid fuels has received considerable attention recently because of increasing interest in the development of carbon neutral energy sources.[1] The production of liquid fuels such as methanol[2] or formic acid[3] from CO_2 and H_2 (or its formal equivalents) is particularly attractive. However, selective production of these products using heterogeneous catalysts remains challenging.[4−6] One interesting approach toward CO_2 reduction is to use molecular catalysis, where product selectivity may be better controlled than heterogeneous systems.[7] The catalytically active species in molecular systems can often be probed either directly or indirectly, thereby offering opportunities to understand the catalytic mechanism and synthetically tune systems in a well-defined manner.[8]

One of the simplest CO_2 reduction reactions is its hydrogenation to formic acid.[3] While a number of noble-metal catalysts for the hydrogenation of CO_2 to formic acid exist,[9−17] there are only a handful of examples using first-row transition metals such as iron[18−24] and cobalt,[25−28] and information about their thermodynamic properties and elementary reaction steps is needed.[29−34] For example, the hydricity (ΔG_{H^-}), which is the heterolytic dissociation energy of $[M–H]^{n+}$ into M^{n+} and H^- (eq 1), has only been experimentally determined for one iron hydride complex (FpH)[35] despite recent reports of iron-catalyzed CO_2 hydrogenation.[18−24] Knowledge of the hydricities of hydrogenation catalysts can aid the design of new catalysts. This is highlighted by the recent work of Linehan and co-workers on a cobalt hydride catalyst,[26,27] in which the design of this efficient CO_2-to-formate hydrogenation system was achieved, in part, by using a cobalt hydride that was more hydridic (i.e., <43 kcal/mol) than the formate[36] (eq 2).

$$[M–H]^{n+} \rightarrow M^{n+1} + H^- \qquad \Delta G_{H^-} \qquad (1)$$

$$OCHO^- \rightarrow CO_2 + H^- \qquad \Delta G_{H^-} = 43\ \text{kcal/mol} \qquad (2)$$

As part of our exploratory research of phosphine-supported iron complexes in small-molecule activation reactions,[37−42] we were interested in studying the catalytic CO_2 hydrogenation chemistry of a series of triphosphinoiron species (Chart 1): $(SiP^R_3)Fe(L)(H)$ (L = H_2 or N_2; SiP^R_3 = $[Si(o\text{-}C_6H_4PR_2)_3]^-$, R = *i*Pr or Ph),[37,43,44] $(PhBP^{iPr}_3)Fe(H)_3(PMe_3)$ ($PhBP^{iPr}_3$ = $PhB(CH_2PiPr_2)_3$),[45] $[(NP^{iPr}_3)Fe(N_2)(H)](PF_6)$ (NP^{iPr}_3 = $N(CH_2CH_2PiPr_2)_3$),[46] $(TPB)(\mu\text{-}H)Fe(L)(H)$ (L = N_2 or H_2; TPB = $B(o\text{-}C_6H_4PiPr_3)_3$),[44] $(CP^{iPr}_3)Fe$ (CP^{iPr}_3 = $[C(o\text{-}C_6H_4PiPr_2)_3]^-$),[42] and $(C^{Si}P^{Ph}_3)Fe$ ($C^{Si}P^{Ph}_3$ = $[C(Si(CH_3)_2CH_2PPh_2)_3]^-$)[47] (Chart 1). These systems are structurally related to two tetraphosphinoiron hydride CO_2 hydrogenation catalysts $([(PP_3)Fe(H_2)(H)](BF_4)$[19,48] and

Special Issue: Small Molecule Activation: From Biological Principles to Energy Applications

Received: October 18, 2014
Published: December 31, 2014

DOI: 10.1021/ic502508p
Inorg. Chem. 2015, 54, 5124−5135

Chart 1. Select Phosphine–Metal Complexes of Relevance to Catalytic CO_2 Hydrogenation

Previous Reports:

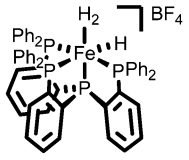

[(tetraphos)Fe(H_2)(H)](BF_4)

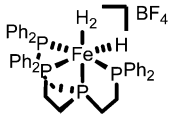

[(PP_3)Fe(H_2)(H)](BF_4)

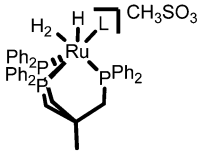

(triphos)Ru(L)(H_2)(H)](CH_3SO_3)

This Report:

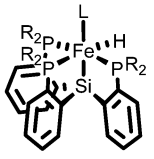

(SiP^R_3)Fe(L)(H)
R = *i*Pr or Ph L = H_2 or N_2

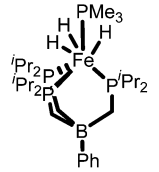

($PhBP^{iPr}_3$)Fe(H)$_3$(PMe_3)

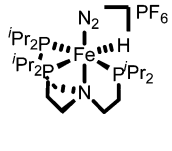

[(NP^{iPr}_3)Fe(N_2)(H)](PF_6)

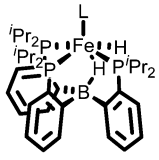

(TPB)(μ-H)Fe(L)(H)
L = H_2 or N_2

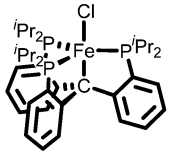

(CP^{iPr}_3)FeCl

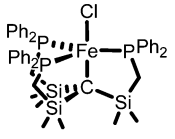

($C^{Si}P^{Ph}_3$)FeCl

(tetraphos)Fe(H_2)(H)](BF_4),[20] where PP_3 = P($CH_2CH_2PPh_2$)$_3$ and tetraphos = P(*o*-$C_6H_4PPh_2$)$_3$), studied in a similar context by the groups of Beller and Laurenczy (Chart 1). A distinguishing feature of the present series of triphosphinoiron complexes is that each of the present ligand scaffolds possesses a different apical unit. These include an X-type silyl in SiP^R_3, an X-type alkyl in (CP^{iPr}_3)Fe and $(C^{Si}P^{Ph}_3)$Fe, a noncoordinating borate in $PhBP^{iPr}_3$, an L-type amine in NP^{iPr}_3, and a Z-type borane in TPB. Each of these apical units can confer different (i) geometries at iron, (ii) formal oxidation states at iron, and (iii) reactivity patterns for otherwise structurally similar species, as we have studied previously with respect to N_2 activation chemistry.[37−42]

In the present work, we experimentally determined the pK_a and hydricity for the (SiP^{iPr}_3)Fe system and studied the catalytic and stoichiometric hydrogenation of CO_2 in this and the related triphosphinoiron species shown in Chart 1. Under elevated temperatures and pressures of CO_2 and H_2 and with triethylamine as the base, the (SiP^{iPr}_3)Fe, (SiP^{Ph}_3)Fe, $(PhBP^{iPr}_3)$Fe, and (CP^{iPr}_3)Fe systems catalytically hydrogenated CO_2 to triethylammonium formate and methylformate, while (NP^{iPr}_3)Fe, (TPB)Fe, and $(C^{Si}P^{Ph}_3)$Fe did not catalyze CO_2 hydrogenation. We also show that despite a low hydricity (i.e., large ΔG_{H^-} value) for the complex (SiP^{iPr}_3)Fe(H_2)(H) (ΔG_{H^-} = 54.3 ± 0.9 kcal/mol) coordination of the formate product to the iron center following hydride transfer to CO_2 provides enough driving force to make the reaction thermally accessible.

RESULTS AND DISCUSSION

pK_a and Hydricity for (SiP^{iPr}_3)Fe. Because Fe–H species have been invoked as intermediates for CO_2 hydrogenation, we were curious if (SiP^{iPr}_3)Fe(H_2)(H) was sufficiently hydridic to react with CO_2. One method for determining hydricities is to use a thermochemical cycle that involves deprotonating the conjugate acid of the metal hydride of interest. We previously reported H_2 chemistry of the (SiP^{iPr}_3)Fe system,[44] including deprotonation of the cationic iron dihydrogen complex [(SiP^{iPr}_3)Fe(H_2)](BAr^F_4) (BAr^F_4 = [(3,5-$(CF_3)_2$–$C_6H_3)_4B]^-$) by Hünig's base under H_2 (1 atm) to afford (SiP^{iPr}_3)Fe(H_2)(H).[43] This motivated us to use this deprotonation reaction to experimentally determine the hydricity of (SiP^{iPr}_3)Fe(H_2)(H) using the series of equations in Scheme 1. The equilibrium in

Scheme 1. Reactions Relevant to Determination of the pK_a and Hydricity of (SiP^{iPr}_3)Fe (B = Base)[a]

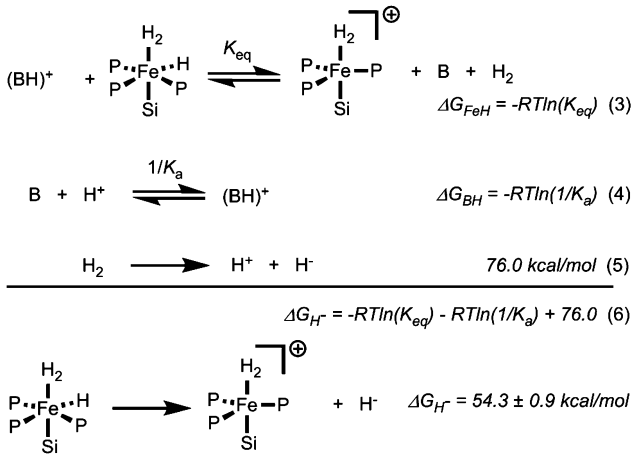

[a]See Chart 1 for a full detailed ligand representation.

eq 3 was followed by ^{1}H NMR spectroscopy independently with 1,8-bis(dimethylamino)naphthalene (proton sponge; K_{eq} = 4.3), 2,6-lutidine (K_{eq} = 3.3 × 10^{-5}), and 2,4,6-trimethylpyridine (K_{eq} = 5.1 × 10^{-5}) in deuterated tetrahydrofuran (THF-d_8). The reverse protonation of (SiP^{iPr}_3)Fe(H_2)(H) with the BAr^F_4 salt of 1,8-bis(dimethylammonium)-naphthalene (K_{eq} = 2.6) was also followed by ^{1}H NMR spectroscopy in THF-d_8.[49]

We note that pK_a of the H_2 ligand in [(SiP^{iPr}_3)Fe(H_2)](BAr^F_4) can be estimated using eqs 3 and 4. The experimentally determined pK_a in THF using this method is pK_a^{THF} = 10.8 ± 0.6 for [(SiP^{iPr}_3)Fe(H_2)](BAr^F_4). Notably, the pK_a^{THF} agrees very well with the predicted value of 10.2 obtained from the ligand acidity constant method recently developed by Morris.[50,51] We caution that this is only a rough estimate of the pK_a of [(SiP^{iPr}_3)Fe(H_2)](BAr^F_4) because the pK_a of [(SiP^{iPr}_3)Fe(H_2)](BAr^F_4) is a measure of the removal of a proton to afford "(SiP^{iPr}_3)Fe(H)", whereas in the observed deprotonation reaction, H_2 coordinates to this species to afford (SiP^{iPr}_3)Fe(H_2)(H) and contributes to the equilibrium depicted in eq 3.

With the equilibrium of eq 3 in hand, the hydricity of the conjugate base (SiP^{iPr}_3)Fe(H_2)(H) can be determined by the summation of eqs 3–5 to give eq 6.[52,53] Most hydricity values have been reported in acetonitrile in part because of the known heterolytic dissociation energy of H_2 in acetonitrile (eq 5). However, irreversible coordination of acetonitrile to [(SiP^{iPr}_3)-Fe(H_2)](BAr^F_4) precluded the use of this solvent. An empirical relationship relates the pK_a^{THF} of a metal complex to the pK_a in acetonitrile (pK_a^{MeCN}).[54] Using this relationship, the pK_a^{MeCN} of [(SiP^{iPr}_3)Fe(H_2)](BAr^F_4) is 15.9 ± 0.7. When the pK_a^{MeCN} of [(SiP^{iPr}_3)Fe(H_2)](BAr^F_4) is combined with eq 5, the hydricity of (SiP^{iPr}_3)Fe(H_2)(H) in MeCN is 54.3 ± 0.9 kcal/mol. To the

DOI: 10.1021/ic502508p
Inorg. Chem. 2015, 54, 5124–5135

best of our knowledge, this is only the second experimentally estimated hydricity value of an iron hydride complex.[35]

Formal hydride transfer from phosphine-ligated iron hydride complexes to CO_2 to give formate is well-known.[29−34,55] A comparison of the hydricity of $(SiP^{iPr}_3)Fe(H_2)(H)$ to that of formate (eq 2) indicates that the reaction for hydride transfer from $(SiP^{iPr}_3)Fe(H_2)(H)$ to CO_2 to afford formate is endergonic by over 10 kcal/mol. Yet, as will be shown below, $(SiP^{iPr}_3)Fe(H_2)(H)$ can still react with CO_2 both stoichiometrically and catalytically to afford formate.

Stoichiometric Reactivity of Fe−H Species with CO_2. In addition to $(SiP^{iPr}_3)Fe(L)(H)$[43,44] (where L = N_2 or H_2), we have previously reported the synthesis and characterization of three other related triphosphinoiron hydride complexes, $(PhBP^{iPr}_3)Fe(H)_3(PMe_3)$,[45] $[(NP^{iPr}_3)Fe(N_2)(H)](PF_6)$,[46] and $(TPB)(\mu\text{-}H)Fe(N_2)(H)$[44] (Chart 1), and demonstrated that the two former complexes, $(PhBP^{iPr}_3)Fe(H)_3(PMe_3)$ and $(TPB)(\mu\text{-}H)Fe(N_2)(H)$, are olefin hydrogenation catalysts. The iron hydride species of the *tris*(diphenylphosphino)silyl ligand, $(SiP^{Ph}_3)Fe(N_2)(H)$, had not previously been reported, but it has now been synthesized in a manner analogous to that of the preparation of the isopropyl analogue $(SiP^{iPr}_3)Fe(N_2)(H)$ (vide infra). The reactivity of these iron hydrides to CO_2 was probed.

Synthesis of Iron Formate Species. A solution of $(SiP^{Ph}_3)Fe(N_2)(H)$ reacted with CO_2 (1 atm) at 50 °C to afford the yellow iron formate species $(SiP^{Ph}_3)Fe(OCHO)$ (Scheme 2a). Consistent with the κ^1-bound formate ligand,[56] attenuated total reflectance infrared (ATR-IR) spectroscopy showed two signature vibrational features at 1618 and 1316 cm^{-1} ($^{13}CO_2$: 1587 and 1254 cm^{-1}) with a $\Delta\nu$(O−C−O) of 302 cm^{-1} (Table 1). As expected for a five-coordinate $(SiP^{R}_3)Fe^{II}$ complex,[57] $(SiP^{Ph}_3)Fe(OCHO)$ is S = 1 (2.7 μ_B in C_6D_6 at RT). Similarly, $(SiP^{iPr}_3)Fe(N_2)(H)$ reacted with CO_2 to afford $(SiP^{iPr}_3)Fe(OCHO)$. The ATR-IR spectrum showed an asymmetric O−C−O stretch at 1623 cm^{-1} ($^{13}CO_2$: 1583 cm^{-1}). While the symmetric O−C−O stretch could not be reliably discerned (Table 1), its S = 1 spin state (2.8 μ_B in C_6D_6 at room temperature (RT)) and yellow color indicate a five-coordinate $(SiP^{iPr}_3)Fe(OCHO)$ complex.

Scheme 2. Stoichiometric CO_2 Hydrogenation to Triethylammonium Formate[a]

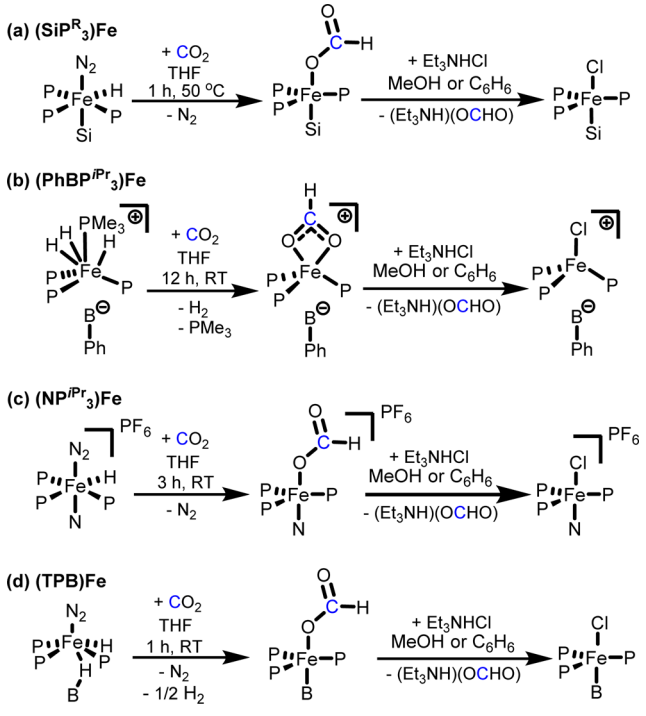

[a]See Chart 1 for detailed representations of the ligands indicated.

Similarly, a THF solution of $(PhBP^{iPr}_3)Fe(H)_3(PMe_3)$ reacted with CO_2 (1 atm) at RT to afford the κ^2-bound formate adduct $(PhBP^{iPr}_3)Fe(OCHO)$ (Scheme 2b). The ATR-IR spectrum of this S = 2 species (5.0 μ_B, C_6D_6 at RT) exhibited features of a formate ligand at 1595 and 1362 cm^{-1} ($^{13}CO_2$: 1546 and 1355 cm^{-1}) with a $\Delta\nu$(O−C−O) = 233 cm^{-1} that is consistent with the κ^2-bound formate assignment.[56] The formate coordination mode is in contrast to the κ^1-bound formate ligands in $(SiP^{R}_3)Fe(OCHO)$, $[(NP^{iPr}_3)Fe(OCHO)](PF_6)$, and $(TPB)Fe(OCHO)$. We presume this arises because of the lower coordination number in $(PhBP^{iPr}_3)Fe$.

A solution of $[(NP^{iPr}_3)Fe(N_2)(H)](PF_6)$ also reacted with CO_2 (1 atm) at RT to afford the formate adduct $[(NP^{iPr}_3)Fe(OCHO)](PF_6)$ (Scheme 2c). $[(NP^{iPr}_3)Fe(OCHO)](PF_6)$ is S = 2 (5.1 μ_B, C_6D_6 at RT), analogous to $[(NP^{iPr}_3)FeCl](PF_6)$,[46] with a diagnostic ν_{asym}(O−C−O) vibrational feature at 1613 cm^{-1} ($^{13}CO_2$: 1579 cm^{-1}) in the ATR-IR spectrum. However, the accompanying lower-energy ν_{sym}(O−C−O) vibrational feature could not be reliably assigned because of overlapping ligand vibrational modes in the 1200−1300 cm^{-1} region. The obscured ν_{sym}(O−C−O) feature prevented assignment of the formate binding mode, but ν_{asym}(O−C−O) most closely matches κ^1-bound formate ligands (Table 1).[56]

Mixing a benzene solution of $(TPB)(\mu\text{-}H)Fe(N_2)(H)$ with CO_2 (1 atm) afforded the κ^1-formate complex (TPB)Fe(OCHO) (Scheme 2d) as a yellow solution. The color, ^1H NMR spectrum, and solution magnetic moment (4.2 μ_B, $S = {}^3/_2$ in C_6D_6 at RT) are consistent with the formulation of (TPB)Fe(OCHO) as a $\{Fe-B\}^7$ species,[58,59] and vibrational modes in the IR spectrum at 1627 and 1291 cm^{-1} ($^{13}CO_2$: 1588 and 1269 cm^{-1}) with a $\Delta\nu$(O−C−O) value of 336 cm^{-1} (Table 1) are diagnostic for a κ^1-formate ligand.[56] The IR spectrum of (TPB)Fe(OCHO) lacks any feature that is diagnostic for a B−H unit.[60] For comparison, in the related S = 2 (TPBH)Fe(CCAr) (Ar = phenyl or tolyl) complex, where a terminal B−H is present, the IR spectra exhibit diagnostic B−H vibrations at 2490 cm^{-1} for Ar = phenyl and 2500 cm^{-1} for Ar = tolyl.[44]

The formation of (TPB)Fe(OCHO) from the reaction of $(TPB)(\mu\text{-}H)Fe(N_2)(H)$ with CO_2 (1 atm) is notable in that there is a formal loss of an hydrogen atom (Schemes 2d and 3). The loss of 0.5 equiv of H_2 (relative to the starting iron complex) was confirmed by gas chromatography with a thermal conductivity detector (GC-TCD; 0.44 equiv of H_2 quantified). The reaction between the previously reported $(TPB)Fe(N_2)$[58] with formic acid also formed (TPB)Fe(OCHO), with 0.42 equiv of H_2 detected by GC-TCD as a product (Scheme 3).

Reactivity of Fe(OCHO) Species. The formate ligands in all five of the aforementioned iron formate complexes are substitutionally labile. The addition of triethylammonium chloride (10 equiv) into either benzene or methanol solutions of these complexes resulted in the formation of the respective iron chloride complexes and triethylammonium formate (Scheme 2). Furthermore, the iron chloride products from these metathesis reactions are synthons for the respective iron hydride complexes.

DOI: 10.1021/ic502508p
Inorg. Chem. 2015, 54, 5124−5135

Table 1. IR Stretching Frequencies and Solution Magnetic Moments for Iron Formate Complexes

		ν_{asym}(O−C−O) (cm^{-1})[b]		ν_{sym}(O−C−O) (cm^{-1})[b]		
	μ_{eff} (μ_B)[a]	CO_2	$^{13}CO_2$	CO_2	$^{13}CO_2$	$\Delta\nu_{asym}$ (O−C−O) (cm^{-1})[c]
(SiP^{Ph}_3)Fe(OCHO)	2.7	1618	1587	1316	1254	302
(SiP^{iPr}_3)Fe(OCHO)	2.8	1623	1583			
($PhBP^{iPr}_3$)Fe(OCHO)	5.0	1595	1546	1362	1355	233
[(NP^{iPr}_3)Fe(OCHO)][PF_6]	5.1	1613	1579			
(TPB)Fe(OCHO)	4.2	1627	1588	1291	1269	336

[a]Solution magnetic moments at RT. [b]ATR-IR data of solution thin films. [c]Difference between ν_{asym}(O−C−O) and ν_{sym}(O−C−O).

Scheme 3. Reactivity of (TPB)Fe Complexes with CO_2 and Formic Acid[a]

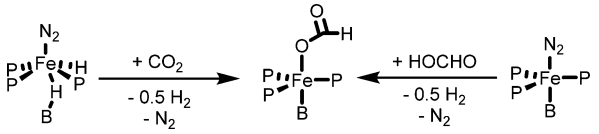

[a]See Chart 1 for a full detailed ligand representation.

With this metathesis reaction and known reaction chemistry for the (SiP^{iPr}_3)Fe scaffold, we can construct a synthetic cycle for CO_2 hydrogenation, which may inform the catalytic CO_2 hydrogenation reaction (vide infra). Starting from the Fe−Cl species, (SiP^{iPr}_3)FeCl reacts with MeMgCl (1 equiv) to afford the iron methyl complex (SiP^{iPr}_3)FeMe (this work, Scheme 4a).

Scheme 4. Synthetic Cycle for CO_2 Hydrogenation to Formate by (SiP^{iPr}_3)Fe[a]

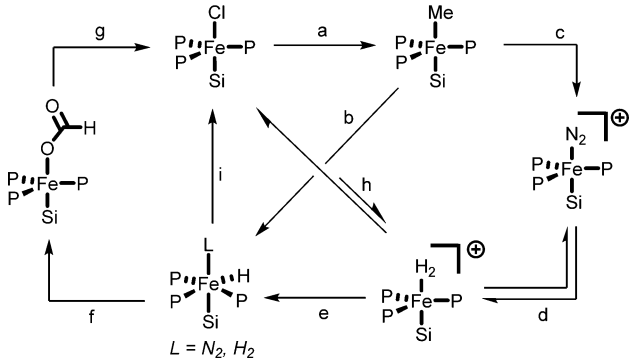

[a]See Chart 1 for a full detailed ligand representation. Conditions: (a) MeMgCl, THF; (b) H_2, THF (plus N_2 workup for L = N_2); (c) ($HBAr^F_4$)(Et_2O)$_2$, C_6H_6; (d) H_2 (forward), N_2 (reverse), THF; (e) Et_3N, THF (plus N_2 workup for L = N_2); (f) CO_2, MeOH, THF, or C_6H_6; (g) (Et_3NH)Cl, C_6H_6 or MeOH; (h) 1 atm:1 atm H_2/D_2, Et_3N, 10:1 CD_3OD/THF-d_8 (HD is produced); (i) for L = N_2, Et_3NHCl, 10:1 CD_3OD/THF-d_8.

Subsequent reaction with H_2 affords (SiP^{iPr}_3)Fe(N_2)(H) (Scheme 4b).[43] Alternatively, the iron methyl complex (SiP^{iPr}_3)FeMe can be converted to the cationic H_2 complex [(SiP^{iPr}_3)Fe(H_2)](BAr^F_4)[43] (Scheme 4c,d). The H_2 ligand in the latter complex can be deprotonated by triethylamine (this work) to generate (SiP^{iPr}_3)Fe(L)(H) (where L = N_2 or H_2; Scheme 4e). As shown above, (SiP^{iPr}_3)Fe(N_2)(H) reacts with CO_2 to afford (SiP^{iPr}_3)Fe(OCHO) (Scheme 4f), which can undergo metathesis with (Et_3NH)Cl to afford the starting iron chloride complex (Scheme 4g).

Reaction of (SiP^{iPr}_3)FeCl with H_2 is also possible. A CD_3OD/THF-d_8 (10:1) solution of (SiP^{iPr}_3)FeCl with excess triethylamine in the presence of H_2 and D_2 (ca. 1 atm:1 atm) gives HD (Scheme 4h). Related, the cationic H_2 adduct [(SiP^{iPr}_3)Fe(H_2)][BAr^F_4], a model for [(SiP^{iPr}_3)Fe(H_2)]$^+$, scrambles a mixture of H_2 and D_2 (ca. 1 atm:1 atm) to HD in a CD_3OD/THF-d_8 solution (10:1). (SiP^{iPr}_3)FeCl is the sole observed iron-containing species by ^{1}H NMR spectroscopy in the former experiment, indicating that the equilibrium with the putative [(SiP^{iPr}_3)Fe(H_2)]$^+$ responsible for scrambling H_2/D_2 heavily favors (SiP^{iPr}_3)FeCl.

Catalytic Hydrogenation. Having realized a synthetic cycle for CO_2 hydrogenation to formate, we explored whether the process could be made catalytic. Following literature precedent, the triphosphinoiron chloride complexes were tested in an initial screen for catalysis,[9−16,18−26,28] and triethylamine was added to serve as a base.[61] ^{1}H NMR spectroscopy with *N*,*N*-dimethylformamide (DMF) added as an integration standard was used to quantify triethylammonium formate yields. Other known products of CO_2 hydrogenation are formate esters such as methylformate that are obtained from the esterification of formate with methanol.[19,20] Because of the volatility and low yields of MeOCHO, GC-FID (GC with flame ionization detection) was used to quantify this product.

Under the standardized reaction conditions of 29 atm of CO_2 and 29 atm of H_2 in a methanol solvent with triethylamine, (SiP^{iPr}_3)FeCl, (SiP^{Ph}_3)FeCl, and ($PhBP^{iPr}_3$)FeCl are precatalysts for hydrogenation of CO_2 to triethylammonium formate and methylformate (Table 2, entries 1−3). (SiP^{Ph}_3)FeCl is the most active, having an average turnover number of 200. These three systems are also more selective for (Et_3NH)(OCHO) than MeOCHO, with ($PhBP^{iPr}_3$)FeCl being the most selective of the three with a 10:1 (Et_3NH)(OCHO) to MeOCHO product ratio. It is also worth noting that the primary coordination sphere of the zwitterionic ($PhBP^{iPr}_3$)Fe system is structurally similar to a known cationic ruthenium system (triphos)Ru (triphos = $CH_3C(CH_2PPh_2)_3$) that hydrogenates CO_2 to methanol[62] and also dehydrogenates formic acid[63] (Chart 1). We have also reported the reduction of CO_2 to oxalate by ($PhBP^{iPr}_3$)Fe.[64]

Under the standard conditions, [(NP^{iPr}_3)FeCl](PF_6) and (TPB)FeCl are not precatalysts for the reaction (Table 2, entries 4 and 5). The recently reported (CP^{iPr}_3)FeCl complex (Chart 1),[42] where the silicon atom in (SiP^{iPr}_3)FeCl is substituted by a carbon atom, is also catalytically competent (Table 2, entry 6) but is significantly less active than (SiP^{Ph}_3)FeCl. Another carbon variant of the triphosphinoiron series of complexes, ($C^{Si}P^{Ph}_3$)FeCl[47] (Chart 1), is not catalytically competent (Table 2, entry 7).

For a direct comparison with known iron CO_2 hydrogenation catalysts and as a benchmark of the method employed, we subjected the (PP_3)Fe[19] and (tetraphos)Fe[20] systems to our standardized conditions. Beller and Laurency reported that a mixture of the PP_3 ligand with Fe(BF_4)$_2$ is one of the more

DOI: 10.1021/ic502508p
Inorg. Chem. 2015, 54, 5124−5135

Table 2. Triphosphinoiron-Catalyzed CO_2 Hydrogenation[a]

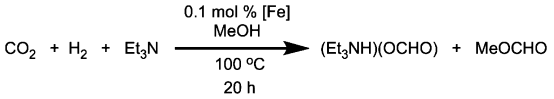

entry	precatalyst	TON[b]	$(Et_3NH)(OCHO)$:MeOCHO ratio[f]
1	$(SiP^{iPr}_3)FeCl$	53	3:1
2	$(SiP^{Ph}_3)FeCl$	200	2:1
3	$(PhBP^{iPr}_3)FeCl$	27	10:1
4	$[(NP^{iPr}_3)FeCl](PF_6)$	0	0
5	(TPB)FeCl	0	0
6	$(CP^{iPr}_3)FeCl$	27	6:1
7	$(C^{Si}P^{Ph}_3)FeCl$	0	0
8	$PP_3/Fe(BF_4)_2$[c,d]	486	3:1
9	$[(tetraphos)FeF]BF_4$[c,e]	1661	1:1
10	$FeCl_2$	0	0
11	$FeCl_2/4PPh_3$	0	0
12	no iron	0	0

[a]Conditions: 0.1 mol % (0.7 mM) iron precatalyst (relative to Et_3N), methanol, 651 mM Et_3N, 29 atm of CO_2 (RT), 29 atm of H_2 (RT), 100 °C, 20 h. [b]Turnover number: combined yield (moles) of $(Et_3NH)(OCHO)$ and MeOCHO divided by moles of precatalyst. [c]Previously studied under slightly different conditions. [d]See ref 19. [e]See ref 20. [f]Ratio of the amount of $(Et_3NH)(OCHO)$ product to the amount of MeOCHO product.

Table 3. $(SiP^{iPr}_3)FeCl$-Catalyzed CO_2 Hydrogenation under Varied Conditions

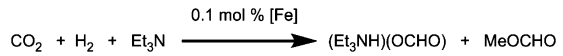

entry	deviation from standard conditions[a]	TON[b]	(Et_3NH) $(OCHO)$:MeOCHO ratio[f]
0	none	53	3:1
1	0 atm of H_2	0	0
2[c]	CD_3OD	32	2:1
3	150 °C	40	2:1
4	20 °C	0	0
5	2 h	16	1:0
6	0.5 equiv of $(Et_3NH)Cl$[d]	41	5:1
7	0.5 equiv of $NaBF_4$[d]	93	6:1
8	0.5 equiv of $NaBAr^F_4$[d]	69	2:1
9	0.5 equiv of NaF[d]	45	8:1
10	0.5 equiv of TBAF[d,e]	33	12:1
11	0.5 equiv of CsF[d]	26	9:1
12	0.5 equiv of K_2CO_3[d]	57	21:1

[a]Standard conditions: 0.1 mol % (0.7 mM) iron precatalyst (relative to Et_3N), methanol, 651 mM Et_3N, 29 atm of CO_2 (RT), 29 atm of H_2 (RT), 100 °C, 20 h. [b]Turnover number: combined yield (moles) of $(Et_3NH)(OCHO)$ and MeOCHO divided by moles of precatalyst. [c]$(Et_3NH)(OCHO)$ was detected by ^1H NMR spectroscopy, but neither $(Et_3ND)(OCDO)$, $(Et_3NH)(OCDO)$, nor $(Et_3ND)(OCHO)$ was detected by ^2H NMR spectroscopy. [d]Relative to moles of $(SiP^{iPr}_3)FeCl$. [e]TBAF = tetrabutylammonium fluoride. [f]Ratio of the amount of $(Et_3NH)(OCHO)$ product to the amount of MeOCHO product.

active conditions for CO_2 hydrogenation in the PP_3 system. Under the standard conditions of this study, a 1:1 mixture of PP_3 and $Fe(BF_4)_2$ hydrogenates CO_2 to triethylammonium formate and methylformate, as well, at a total TON of 486 (Table 2, entry 8). The $(tetraphos)Fe(F)(BF_4)_2$ complex also catalyzes CO_2 hydrogenation to the same products at a total TON of 1661 (Table 2, entry 9). These values are in near agreement with the respective literature reports. The $(tetraphos)Fe(F)(BF_4)_2$ complex is the least selective of the series in Table 2 for formate production.

A series of control experiments were performed to probe the homogeneity of the reaction. The catalytic reaction is uninhibited by the addition of elemental mercury (see the Supporting Information, SI). Also, CO_2 hydrogenation does not occur with the iron salt $FeCl_2$ (Table 2, entry 10) or with a 1:4 mixture of $FeCl_2$ and triphenylphosphine (Table 2, entry 11), nor does it proceed in the absence of an iron source (Table 2, entry 12). These experiments do not preclude a role for heterogeneous species but provide evidence consistent with a homogeneous process.

To gain insight into the reaction, we chose to study the hydrogenation catalysis by the $(SiP^{iPr}_3)Fe$ system further because it is more active than $(PhBP^{iPr}_3)FeCl$ and because its coordination chemistry has been studied in greater detail than that of its phenyl analogue $(SiP^{Ph}_3)Fe$.[43,44]

Under standard conditions but in the absence of H_2, triethylammonium formate and methylformate were not detected (Table 3, entry 1). Furthermore, when the reaction was run in CD_3OD instead of CH_3OH, $(Et_3NH)(OCHO)$ was detected by ^1H NMR spectroscopy at the conclusion of the reaction, while $(Et_3ND)(OCDO)$ was not detected by ^2H NMR spectroscopy (Table 3, entry 2). The data collectively indicate that H_2 is the source of the hydrogen atom equivalents.

High pressures of CO_2 and H_2 are critical because the reaction does not proceed at or near atmospheric pressures of H_2 and CO_2 (see the SI) in agreement with most literature examples.[3,9−16,19−26,28] Milstein and co-workers have reported CO_2 hydrogenation to formate at a relatively low 10 total atm of H_2 and CO_2.[18] Also critical is methanol because the catalytic activity does not occur in neat THF under any pressures of CO_2 and H_2 studied here (see the SI), highlighting the importance of polar, protic solvents in phosphinoiron CO_2 hydrogenation catalysis.[61]

It was determined that 100 °C and 20 h are optimal for the reaction under the conditions studied here. Running the reaction at 150 °C slightly reduces the turnover relative to the standard conditions (Table 3, entry 3), which is likely a result of catalyst decomposition (vide infra). At 20 °C, no reaction occurs (Table 3, entry 4), and the starting precatalyst $(SiP^{iPr}_3)FeCl$ is the only iron-containing species at the end of the reaction. Reducing the reaction time to 2 h at 100 °C reduces the TON by a factor of 3 (Table 3, entry 5) compared to the standard conditions.

Using the stoichiometric reactions as a guide, we also probed the effects of additives and precatalysts on the catalysis. The stoichiometric metathesis reaction for the transformation of $(SiP^{iPr}_3)Fe(OCHO)$ to $(SiP^{iPr}_3)FeCl$ suggests that chloride substitution for formate may be a route for formate release. However, the addition of 0.5 equiv of $(Et_3NH)Cl$ (relative to iron) into the reaction reduces the TON, although the selectivity for $(Et_3NH)(OCHO)$ over MeOCHO slightly increases to 5:1 (Table 3, entry 6). It appears that while chloride may substitute for formate, excess chloride may also slow H_2 substitution at iron (vide infra) and reduces the overall TON. The addition of a noncoordinating anion in the form of $NaBF_4$ to the catalytic mixture is beneficial, yielding a TON of 93 and 6:1 selectivity for $(Et_3NH)(OCHO)$ (Table 3, entry 7), while the addition of $Na(BAr^F_4)$ only modestly increases the TON to 69 and without significantly affecting the selectivity

DOI: 10.1021/ic502508p
Inorg. Chem. 2015, 54, 5124−5135

(Table 3, entry 8). The origin of the effect from the Na^+ and/or borate anion is not understood, but one effect may be that Na^+ facilitates removal of the inner-sphere chloride as NaCl. Additionally, alkali metals are known to facilitate CO_2 coordination to cobalt centers.[65] It is also noteworthy that BF_4^- is the counteranion of the highly active tetraphosphinoiron $(PP_3)Fe$[19] and (tetraphos)Fe[20] systems and is also beneficial for iron-catalyzed formic acid dehydrogenation.[66] It is unlikely that fluoride, which may be a decomposition product of BF_4^-, is the source of the positive response because fluoride salts decrease the TON but increase the selectivity for (Et_3NH)-(OCHO) (Table 3, entries 9–11). Finally, the addition of K_2CO_3, which has been reported to enhance CO_2 hydrogenation catalysis for some noble- and non-noble-metal systems,[67] has no effect on the TON but significantly increases the selectivity for $(Et_3NH)(OCHO)$ compared to the other additives (Table 3, entry 12). The additives containing coordinating anions are more selective for $(Et_3NH)(OCHO)$ over MeOCHO, presumably a result of anion coordination inhibiting iron-catalyzed esterification of formate to methylformate.[68] However, we caution that these results are qualitative. A systematic study of the effects of these and other additives on catalysis would be warranted to draw quantitative conclusions.

Other important factors known to affect catalysis are the base identity[26] and base concentrations.[61] A careful study of the effect of different bases and concentrations on catalysis in the present series is beyond the scope of this report, but we point out that the pK_a of triethylamine is suitably matched to the pK_a of $[(SiP^{iPr}_3)Fe(H_2)]^+$ (vide supra), an intermediate in the catalytic cycle of the $(SiP^{iPr}_3)Fe$ system (Scheme 5; vide infra).

Other $(SiP^{iPr}_3)Fe$ species are also competent precatalysts. The iron formate $(SiP^{iPr}_3)Fe(OCHO)$ and iron hydride complex $(SiP^{iPr}_3)Fe(N_2)(H)$ are each catalytically competent precatalysts (Table 4, entries 1 and 2), with TONs comparable to that of $(SiP^{iPr})FeCl$. The cationic N_2 complex $[(SiP^{iPr}_3)Fe(N_2)](BAr^F_4)$, which is a synthon for $(SiP^{iPr}_3)Fe(N_2)(H)$ in the presence of H_2 and triethylamine (Scheme 4), is also a catalytically competent precatalyst (Table 4, entry 3). Finally, a 1:1 mixture of the free ligand $HSiP^{iPr}_3$ and $FeCl_2$ is significantly less catalytically competent than the synthesized iron complex $(SiP^{iPr}_3)FeCl$ (Table 4, entry 4). All four of these precatalysts are more selective than $(SiP^{iPr}_3)FeCl$ for $(Et_3NH)(OCHO)$.

We also probed the fate of the iron precatalyst $(SiP^{iPr}_3)FeCl$ under the reaction conditions. At the end of the reaction under standard conditions, the ^{31}P NMR spectrum showed a mixture of phosphorus-containing material, including significant quantities of free ligand $(HSiP^{iPr}_3)$. If the reaction was run at RT, only the starting precatalyst $(SiP^{iPr}_3)FeCl$ was observed by ^1H NMR spectroscopy. These observations indicate that while the catalysis requires heating, elevated temperatures lead to eventual catalyst decomposition.

A possible catalytic cycle based in part on the observed stoichiometric reactions discussed in Scheme 4 is proposed in Scheme 5 for the $(SiP^{iPr}_3)Fe$ system. Starting from precatalyst $(SiP^{iPr}_3)FeCl$ in Scheme 5, H_2 substitution forms the cationic H_2 adduct $[(SiP^{iPr}_3)Fe(H_2)]^+$. The viability of this H_2 for Cl^- substitution step is demonstrated by H/D scrambling experiments discussed above. However, we cannot rule out a process wherein methanol is involved in the displacement of Cl^- through, for example, methanol for Cl^- substitution at iron followed by H_2 substitution of methanol. The cationic H_2 adduct $[(SiP^{iPr}_3)Fe(H_2)]^+$ in the catalytic cycle can be deprotonated by triethylamine to give $(SiP^{iPr}_3)Fe(H_2)(H)$, as we have observed in the stoichiometric reaction (Scheme 4e). The reverse of this reaction is also possible: a 1:1 mixture of $(Et_3NH)Cl$ and $(SiP^{iPr}_3)Fe(H_2)(H)$ reacts to afford (SiP^{iPr}_3)-FeCl (Scheme 4i).

The iron hydride intermediate $(SiP^{iPr}_3)Fe(H_2)(H)$ can then react with CO_2 to form the iron formate complex $(SiP^{iPr}_3)Fe$-(OCHO), which can subsequently react with $(Et_3NH)Cl$, reform $(SiP^{iPr}_3)FeCl$, and release $(Et_3NH)(OCHO)$. The direct conversion of $(SiP^{iPr}_3)Fe(OCHO)$ to $[(SiP^{iPr}_3)Fe(H_2)]^+$ may also be a viable pathway because chloride-free $[(SiP^{iPr}_3)$-$Fe(N_2)](BAr^F_4)$, $(SiP^{iPr}_3)Fe(N_2)(H)$, and $(SiP^{iPr}_3)Fe(OCHO)$ are catalytically competent.

An alternative mechanism involving an iron dihydride species cannot be ruled out but is unlikely for the $(SiP^{iPr}_3)Fe$ system (Scheme 6a). A similar mechanism was proposed by Beller et al. for the cationic (tetraphos)Fe catalyst based on in situ NMR data, where the intermediate $[(tetraphos)Fe(H_2)(H)]^+$ was deprotonated by Et_3N to give $(tetraphos)Fe(H)_2$ (Scheme 6b).[20] This iron dihydride intermediate was suggested to react

Table 4. CO_2 Hydrogenation Catalyzed by Various (SiP^{iPr}_3)Fe Species[a]

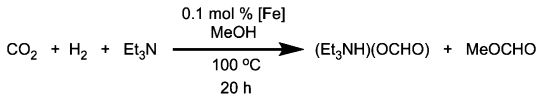

entry	precatalyst	TON[b]	$(Et_3NH)(OCHO)$:MeOCHO ratio[d]
0	$(SiP^{iPr}_3)FeCl$	53	3:1
1	$(SiP^{iPr}_3)Fe(OCHO)$	52	15:1
2	$(SiP^{iPr}_3)Fe(N_2)(H)$	47	3:1
3	$[(SiP^{iPr}_3)Fe(N_2)](BAr^F_4)$	18	8:1
4	$HSiP^{iPr}_3/FeCl_2$ (1:1)[c]	12	4:1

[a]Conditions: 0.1 mol % (0.7 mM) iron precatalyst (relative to Et_3N), methanol, 651 mM Et_3N, 29 atm of CO_2 (RT), 29 atm of H_2 (RT), 100 °C, 20 h. [b]Turnover number: combined yield (moles) of $(Et_3NH)(OCHO)$ and MeOCHO divided by moles of precatalyst. [c]1:1 mixture of $HSiP^{iPr}_3$:$FeCl_2$ (0.7 mM) was used as the precatalyst in place of $(SiP^{iPr}_3)FeCl$. [d]Ratio of the amount of $(Et_3NH)(OCHO)$ product to the amount of MeOCHO product.

Scheme 5. Proposed Catalytic Cycle for $(SiP^{iPr}_3)Fe$ in MeOH[a]

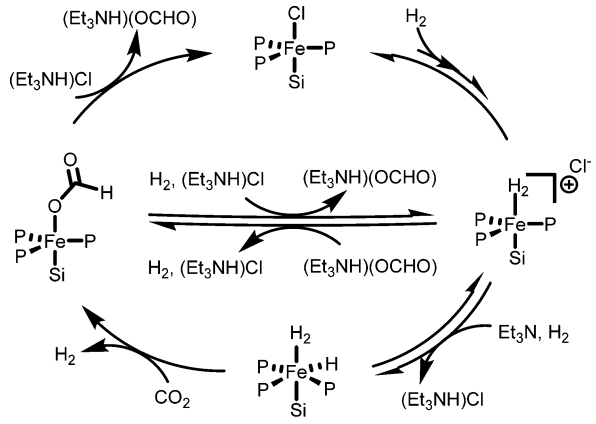

[a]See Chart 1 for a full detailed ligand representation.

DOI: 10.1021/ic502508p
Inorg. Chem. 2015, 54, 5124–5135

Scheme 6. Dihydride Pathways for Catalytic CO_2 Hydrogenation[a]

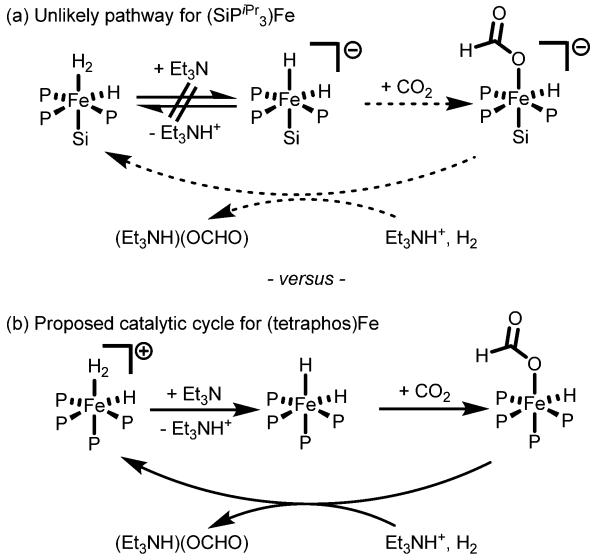

[a]See Chart 1 for a full detailed representation of the ligands indicated.

with CO_2 to give the iron hydride formate intermediate (tetraphos)Fe(H)(OCHO). However, we note that a dihydride intermediate in the (SiP$^{iPr}_3$)Fe system would be unlikely because the analogous deprotonaton of (SiP$^{iPr}_3$)Fe(H$_2$)(H) would form an anionic iron dihydride species "[(SiP$^{iPr}_3$)Fe(H)$_2$]$^-$", which is likely to be thermodynamically inaccessible. For example, a solution of (SiP$^{iPr}_3$)Fe(H$_2$)(H) with excess triethylamine is stable for hours at 90 °C. While this does not rule out the possibility of an equilibrium mixture of (SiP$^{iPr}_3$)Fe(H$_2$)(H) and [(SiP$^{iPr}_3$)Fe(H$_2$)]$^-$, heavily favoring the neutral monohydride species, we also note that the estimated pK_a of the H$_2$ and H$^-$ ligands in (SiP$^{iPr}_3$)Fe(H$_2$)(H) is greater than 45 in THF,[51] vastly higher than that for triethylamine ([Et$_3$NH]$^+$; pK_a = 12.5 in THF).[69]

It is of interest to compare the (SiP$^R_3$)Fe system to the catalytically incompetent (TPB)Fe system because (TPB)(μ-H)Fe(N$_2$)(H) is an olefin hydrogenation catalyst.[44] A key step that may be required for catalysis is the substitution of Cl$^-$ by H$_2$ in (SiP$^{iPr}_3$)FeCl to give the cationic H$_2$ adduct [(SiP$^{iPr}_3$)Fe(H$_2$)]$^+$. Deprotonation of the H$_2$ ligand in a C$_6$D$_6$/THF-d_8 mixture by triethylamine leads to the CO_2-reactive iron hydride complex (SiP$^{iPr}_3$)Fe(H$_2$)(H). The initial H$_2$ substitution step, therefore, is critical towards forming (SiP$^{iPr}_3$)Fe(H$_2$)(H). However, the {Fe–B}^{7} complexes (TPB)Fe(OCHO) and (TPB)FeCl do not react with H$_2$ (4 atm). Related, the previously reported {Fe–B}^{7} [(TPB)Fe](BAr$^F_4$) complex,[41] which has a vacant fifth coordination site, does not react with H$_2$ in the presence of excess triethylamine under 1 atm of H$_2$ at 90 °C for 12 h. Furthermore, [(TPB)Fe](BAr$^F_4$) does not hydrogenate CO_2 under the catalytic conditions (see the SI). [(NP$^{iPr}_3$)FeCl](PF$_6$) is not a hydrogenation precatalyst for possibly the same reason. Qualitatively, it appears that the inability of these latter systems to coordinate H$_2$, presumably a reflection of their weaker ligand-field strengths by comparison to the SiP$^R_3$ system and hence their tendency to populate high-spin configurations ([(NP$^{iPr}_3$)FeCl](PF$_6$), S = 2;[46] (TPB)FeCl, S = $^3/_2$[58]), limits their efficacy toward CO_2 hydrogenation by comparison with the (SiP$^R_3$)Fe system [(SiP$^{iPr}_3$)FeCl; S = 1[57]]. An additional factor preventing catalysis in the (TPB)Fe system is the unproductive loss of 0.5 equiv of H$_2$ following the reaction of (TPB)(μ-H)Fe(N$_2$)(H) with CO_2, which generates the catalytically incompetent (TPB)Fe(OCHO) (Scheme 3).

Influence of the Hydricity on the Reaction with CO_2. On the basis of only the hydricity (54.3 ± 0.9 kcal/mol), the reaction of (SiP$^{iPr}_3$)Fe(H$_2$)(H) with CO_2 to afford formate (ΔG_{H^-} = 43 kcal/mol) is endergonic by over 10 kcal/mol. However, comparisons of only the hydricities of the iron hydride and formate neglect to take into account the observed formate coordination to iron (Scheme 2). To estimate the free energy afforded by formate coordination to iron, we determined the formate binding constant by UV–vis titration for the reaction of [(SiP$^{iPr}_3$)Fe(N$_2$)](BAr$^F_4$) and Li(OCHO) to (SiP$^{iPr}_3$)Fe(OCHO) (Scheme 7, eq 7). The titration in THF

Scheme 7. Gibbs Free Energies for the Reactions of Relevance to CO_2 Hydrogenation by (SiP$^{iPr}_3$)Fe(H$_2$)(H)[a]

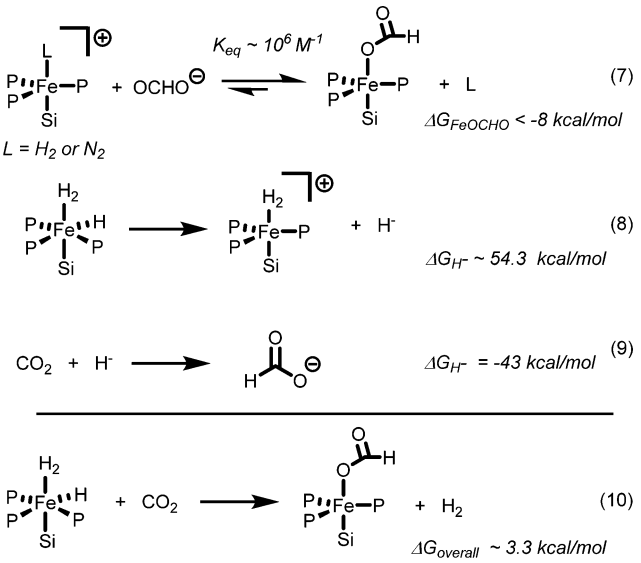

[a]See Chart 1 for a full detailed ligand representation.

indicates that the binding constant of formate to the iron complex is on the order of 10^6 M^{-1}. This is equivalent to ΔG < −8 kcal/mol for formate binding. Thus, the added driving force from formate coordination brings the free-energy change for the reaction of (SiP$^{iPr}_3$)Fe(H$_2$)(H) and CO_2 to form (SiP$^{iPr}_3$)Fe(OCHO) to about 3 kcal/mol (Scheme 7, eq 10; from the sum of eqs 7–9). This is thermally accessible at the elevated temperatures at which the stoichiometric and catalytic reactions are run.

We caution that (SiP$^{iPr}_3$)Fe(H$_2$)(H) may not be the actual iron hydride intermediate that reacts with CO_2; i.e., an intermediate elementary step may occur prior to CO_2 reacting with the iron complex. The hydricity of such a species is likely different from that of (SiP$^{iPr}_3$)Fe(H$_2$)(H) owing to the trans-influencing Si$^-$. We also note that these hydricity values are for acetonitrile, while the catalytic reactions were run in methanol. The magnitude of the difference in hydricities between formate and metal hydrides is known to decrease upon a change from acetonitrile to water.[70] A similar phenomenon may be occurring in methanol, where the difference in the hydricity between (SiP$^{iPr}_3$)Fe(H$_2$)(H) and formate may not be as large as the values in acetonitrile. This, combined with formate coordination to iron (Scheme 7, eq 7), may, in fact, make this formal CO_2 insertion step exergonic in methanol.

DOI: 10.1021/ic502508p
Inorg. Chem. 2015, 54, 5124–5135

CONCLUSIONS

In summary, we studied a series of triphosphinoiron hydride complexes, including $(SiP^{R}_3)Fe(L)(H)$, $(PhBP^{iPr}_3)Fe(H)_3(PMe_3)$, $[(NP^{iPr}_3)Fe(N_2)(H)](PF_6)$, and $(TPB)(\mu\text{-}H)Fe(N_2)(H)$ in the context of CO_2 hydrogenation. These iron hydride complexes react with CO_2 to afford iron formate complexes, which can undergo metathesis with triethylammonium chloride to release triethylammonium formate and well-defined iron chloride complexes, which are themselves synthons for the CO_2-reactive iron hydride complexes (Scheme 2). Subjecting these iron complexes to catalytic conditions under elevated pressures of H_2 and CO_2, we found that $(SiP^{iPr}_3)FeCl$, $(SiP^{Ph}_3)FeCl$, and $(PhBP^{iPr}_3)FeCl$ are precatalysts for catalytic CO_2 hydrogenation to formate and methylformate (Table 2). $(CP^{iPr}_3)FeCl$, in which carbon replaces the silicon atom in $(SiP^{iPr}_3)FeCl$, was also a competent catalyst. The catalytic reactions proceeded in methanol but not in THF, highlighting the importance of solvent in the catalytic reaction.[61]

As depicted in Scheme 5, we believe that H_2 substitution into $(SiP^{iPr}_3)FeCl$ or $(SiP^{iPr}_3)Fe(OCHO)$ to form $[(SiP^{iPr}_3)Fe(H_2)]^+$ followed by deprotonation to form the CO_2-reactive $(SiP^{iPr}_3)Fe(H_2)(H)$ are key steps in the catalytic cycle and determine catalytic competency. The proposed mechanism for $(SiP^{iPr}_3)Fe$ also differs from the mechanism for the highly active (tetraphos)Fe system, which proceeds through a dihydride intermediate.

Finally, the hydricity value of an iron hydride species has also been experimentally determined. The hydricity of $(SiP^{iPr}_3)Fe(H_2)(H)$ is 54.3 ± 0.9 kcal/mol in acetonitrile, and the estimated pK_a^{MeCN} of the related conjugate acid $[(SiP^{iPr}_3)Fe(H_2)](BAr^F_4)$ is 15.9 ± 0.7. Despite the low hydricity, $(SiP^{iPr}_3)Fe(H_2)(H)$ hydrogenates CO_2 to formate, and part of the driving force for the reaction is coordination of formate to the iron center. Thus, the free-energy change for the reaction between $(SiP^{iPr}_3)Fe(H_2)(H)$ and CO_2 to $(SiP^{iPr}_3)Fe(OCHO)$ is only slightly uphill at 3 kcal/mol and accessible under the reactions conditions. It will be of interest to measure the hydricities of other iron hydrides, including within the present series of complexes, in the context of CO_2 hydrogenation to better understand the factors that may lead to improved catalytic activity.

EXPERIMENTAL SECTION

General Considerations. All manipulations were carried out using standard glovebox or Schlenk techniques under an N_2 atmosphere. Unless otherwise noted, solvents were deoxygenated and dried by thorough sparging with N_2 gas followed by passage through an activated alumina column in the solvent purification system by SG Water, USA LLC, Nashua, NH. Deuterated solvents and $^{13}CO_2$ gas were purchased from Cambridge Isotope Laboratories, Inc., Tewksbury, MA. The deuterated solvents were degassed and dried over activated 3 Å sieves prior to use. Unless otherwise noted, all compounds were purchased commercially and used without further purification. $(SiP^{iPr}_3)Fe(N_2)(H)$,[43] $(SiP^{iPr}_3)FeCl$,[57] $[(SiP^{iPr}_3)Fe(N_2)](BAr^F_4)$,[37] $(SiP^{Ph}_3)FeCl$,[57] $(SiP^{Ph}_3)FeMe$,[57] $(PhBP^{iPr}_3)Fe(H)_3(PMe_3)$,[45] $(PhBP^{iPr}_3)FeCl$,[38] $[(NP^{iPr}_3)Fe(N_2)(H)](PF_6)$,[46] $[(NP^{iPr}_3)FeCl](PF_6)$,[46] $(TPB)(\mu\text{-}H)Fe(N_2)(H)$,[44] $(CP^{iPr}_3)FeCl$,[42] and $(C^{Si}P^{Ph}_3)FeCl$[47] were synthesized by literature procedures. Elemental analyses were performed by Robertson Microlit Laboratories, Ledgewood, NJ.

NMR spectra were recorded on Varian 300, 400, and 500 MHz spectrometers. ^1H and ^{13}C chemical shifts are reported in ppm relative to residual solvent as internal standards. ^{31}P and ^{11}B chemical shifts are reported in ppm relative to 85% aqueous H_3PO_4 and $BF_3{\cdot}Et_2O$, respectively. Multiplicities are indicated by br (broad), s (singlet), d (doublet), t (triplet), quart (quart), quin (quintet), multiplet (m), d−d (doublet of doublets), and t−d (triplet of doublets).

The ATR-IR measurements were performed in a glovebox on a thin film of the complex obtained from evaporation of a drop of the solution on the surface of a Bruker APLHA ATR-IR spectrometer probe (Platinum Sampling Module, diamond, *OPUS* software package) at 2 cm^{-1} resolution. IR intensities indicated by s (strong), m (medium), and w (weak).

UV−vis spectra were collected on a Cary 60 UV−vis spectrophotometer. The titration experiments were performed in a glovebox using an Ocean Optics HR4000CG spectrometer.

H_2 Quantification by GC-TCD. H_2 was quantified on an Agilent 7890A gas chromotograph (HP-PLOT U, 30 m, 0.32 mm i.d.; 30 °C isothermal; 1 mL/min flow rate; helium carrier gas) using a thermal conductivity detector. The total amount of H_2 produced was determined as the sum of H_2 in the headspace plus dissolved H_2 in the solution calculated by Henry's law with a constant of 328 MPa.[71]

Methylformate Quantification by GC-FID. Methylformate quantification was performed on a 1.2 mL aliquot of the crude reaction mixture by GC-FID against a methylformate calibration curve. GC-FID instrument: Hewlett-Packard 5890 with a 57 m Restek RTX-VRX column (0.32 mm i.d., 1.8 μm films). Method parameters: helium carrier gas, 1 μL injection volume, 200 °C inlet temperature, 250 °C detector temperature, 7:1 split ratio, 2.9 mL/min flow rate, 20 psi pressure, 35 cm/s velocity. Ramp rate: 35 °C initial temperature held for 8 min, followed by 10 °C/min steps up to 100 °C, then immediately followed by 25 °C/min steps up to 230 °C, which was held for 4 min.

Synthetic Protocols. *Synthesis of $(SiP^{iPr}_3)FeMe$ from $(SiP^{iPr}_3)FeCl$.* A yellow solution of $(SiP^{iPr}_3)FeCl$ (44.4 mg, 73 μmol) in THF (10 mL) was cooled to −78 °C. A solution of MeMgCl (24 μL of a 3 M THF solution, 73 μmol) was diluted with THF (1 mL) and then added dropwise to the stirring reaction, causing a gradual change to a red solution. The stirring solution was allowed to warm to RT overnight. The crude mixture was filtered through a glass frit to remove black precipitate, and the volatiles were removed in vacuo to reveal a red solid. The material was taken up in a minimal amount of pentane and allowed to sit at −35 °C overnight, revealing red crystals of $(SiP^{iPr}_3)FeMe$ (11.3 mg, 22%). The ^1H and ^{31}P NMR spectra of this material were identical with the reported spectra.[57]

Synthesis of $(SiP^{iPr}_3)Fe(OCHO)$. A yellow THF solution (10 mL) of $(SiP^{iPr}_3)Fe(N_2)(H)$ (50 mg, 72 μmol) was degassed by freeze−pump−thaw cycles (3×). Subsequently, CO_2 (1 atm) was introduced to the thawed solution. The reaction was sealed and then heated for 1 h at 50 °C to give a yellow solution. The volatiles were removed in vacuo to give a yellow solid. The material was extracted with C_6H_6 and lyophilized to give $(SiP^{iPr}_3)Fe(OCHO)$ as a yellow solid (46 mg, 90%). Analytically pure material was obtained by layering a concentrated solution of $(SiP^{iPr}_3)Fe(OCHO)$ in THF (1 mL) under HMDSO (5 mL) and allowing the solution to sit at −35 °C for 3 days. ^1H NMR (C_6D_6, 400 MHz): δ 12.2, 12.1, 4.7, 4.6, 1.3, 0.2, −2.0, −2.2, −4.9. μ_{eff} (C_6D_6, method of Evans, 20 °C): 2.8 μ_B (S = 1). IR (thin film, cm^{-1}): 1623 (m, ν_{asym}(O−C−O)). UV−vis (THF, nm {M^{-1} cm^{-1}}): 357 {shoulder, 3247}, 426 {2243}, 478 {253}, 963 {br abs starting at 884 nm, 451}. Anal. Calcd for $C_{37}H_{55}FeO_2P_3Si$: C, 62.71; H, 7.82. Found: C, 61.81; H, 7.24.

Synthesis of $(SiP^{iPr}_3)Fe(O^{13}CHO)$. The procedures used to synthesize $(SiP^{iPr}_3)Fe(OCHO)$ were used here, except that $^{13}CO_2$ was used in place of CO_2. The ^1H NMR spectrum was identical with that of $(SiP^{iPr}_3)Fe(OCHO)$. IR (thin film, cm^{-1}): 1583 (m, $\nu_{asym}(O-{}^{13}C-O)$).

Synthesis of $(SiP^{Ph}_3)Fe(N_2)(H)$. A procedure nearly identical with that used to synthesize $(SiP^{iPr}_3)Fe(N_2)(H)$ was used to synthesize $(SiP^{Ph}_3)Fe(N_2)(H)$. In a 100 mL Schlenk tube, a red solution of $(SiP^{Ph}_3)FeMe$ (26.3 mg, 30 μmol) in THF (20 mL) was degassed by freeze−pump−thaw cycles (3×). H_2 gas (1 atm) was charged into the thawed solution. The reaction was then sealed and heated to 60 °C for over 1 week. The reaction was then filtered through Celite, and

DOI: 10.1021/ic502508p
Inorg. Chem. 2015, 54, 5124−5135

volatiles were removed in vacuo to give a light-yellow powder. The solid was collected on a glass frit and washed with pentane (3 mL × 2). The resulting product (SiP^{Ph}_3)Fe(N_2)(H) (24.4 mg, 91%) was obtained as a light-yellow powder after drying under vacuum. Layering a THF solution of (SiP^{Ph}_3)Fe(N_2)(H) under Et_2O and letting the solution stand for 2 days yielded an analytically pure powder of (SiP^{Ph}_3)Fe(N_2)(H). ^{1}H NMR (C_6D_6, 300 MHz): δ 8.55 (2H, d, $^2J_{H-H}$ = 6 Hz, Ar−*H*), 8.32 (2H, d, $^2J_{H-H}$ = 3 Hz, Ar−*H*), 7.62 (3H, br s, Ar−*H*), 7.45 (2H, br s, Ar−*H*), 7.34 (4H, d, $^2J_{H-H}$ = 6 Hz, Ar−*H*), 6.85 (2H, t, $^2J_{H-H}$ = 6 Hz, Ar−*H*), 6.69 (3H, q, $^2J_{H-H}$ = 3 Hz, Ar−*H*), 6.52 (2H, q, $^2J_{H-H}$ = 3 Hz, Ar−*H*), −11.88 (1H, t-d, $^2J_{P_{cis}-H}$ = 54 Hz, $^2J_{P_{trans}-H}$ = 12 Hz, Fe−*H*). ^{31}P NMR (C_6D_6, 121 MHz): δ 85.3 (2P, s), 78.7 (1P, s). ^{13}C NMR (THF with 1 drop of C_6D_6, 125 MHz): δ 156.3 (d, J_{C-P} = 38 Hz, C^{Ar}), 155.8 (d, J_{C-P} = 35 Hz, C^{Ar}), 150.7 (d, J_{C-P} = 5 Hz, C^{Ar}), 150.4 (s, C^{Ar}), 150.2 (s, C^{Ar}), 143.0 (s, C^{Ar}), 141.6 (d, *J* = 23 Hz, C^{Ar}), 141.0 (s, C^{Ar}), 139.6 (d, *J* = 28 Hz, C^{Ar}), 138.6 (d, *J* = 10 Hz, C^{Ar}), 133.8 (s, C^{Ar}), 132.6 (s, C^{Ar}), 132.3 (s, C^{Ar}), 129.5 (s, C^{Ar}), 128.4 (s, C^{Ar}), 128.2 (s, C^{Ar}), 128.1 (s, C^{Ar}), 127.5 (d, *J* = 5 Hz, C^{Ar}). IR (thin film, cm^{-1}): 2073 (s, ν(N−N)), 1889 (w, ν(Fe−H)). UV−vis (THF, nm {M^{-1} cm^{-1}}): 335 {shoulder, 8125}, 437 {shoulder, 4500}. Anal. Calcd for $C_{54}H_{43}FeN_2P_3Si$: C, 72.32; H, 4.83; N, 3.12. Found: C, 72.94; H, 5.22; N, 2.83.

Synthesis of (SiP^{Ph}_3)Fe(OCHO). A yellow THF solution (10 mL) of (SiP^{Ph})Fe(N_2)(H) (51 mg, 57 μmol) was degassed by freeze−pump−thaw cycles (3×). CO_2 (1 atm) was introduced to the thawed solution. The reaction was sealed and then heated for 1 h at 50 °C to give a yellow solution. The volatiles were removed in vacuo to give a yellow solid. The material was redissolved in C_6H_6 and filtered through a pipet filter to remove a small amount of black material. The filtrate was lyophilized in vacuo to give (SiP^{Ph}_3)Fe(OCHO) as a yellow solid (41 mg, 79%). Analytically pure material was obtained by layering a concentrated THF solution of (SiP^{Ph}_3)Fe(OCHO) (3 mL) under pentane (5 mL) and allowing it to stand for 2 days at RT. ^{1}H NMR (3:2 mixture of C_6D_6/THF-d_8, 300 MHz): δ 12.2, 6.5, 5.7, 4.8, −2.1, −4.7. μ_{eff} (THF-d_8, method of Evans, 20 °C): 2.7 μ_B (*S* = 1). IR (thin film, cm^{-1}): 1618 (m, ν_{asym}(O−C−O)), 1316 (m, ν_{sym}(O−C−O)). UV−vis (THF, nm {M^{-1} cm^{-1}}): 325 {shoulder, 4775}, 415 {4100}, 474 {3700}, 995 {br abs starting at 900 nm, 263}. Anal. Calcd for $C_{55}H_{43}FeO_2P_3Si$: C, 72.37; H, 4.75. Found: C, 73.21; H, 5.48.

Synthesis of (SiP^{Ph}_3)Fe(O^{13}CHO). The same procedures as those used to synthesize (SiP^{Ph}_3)Fe(OCHO) were used here, except that $^{13}CO_2$ was used in place of CO_2. The ^{1}H NMR spectrum of (SiP^{Ph}_3)Fe(O^{13}CHO) was identical with that of (SiP^{Ph}_3)Fe(OCHO). IR (thin film, cm^{-1}): 1587 (m, ν_{asym}(O−^{13}C−O)), 1254 (m, ν_{sym}(O−^{13}C−O)).

Synthesis of ($PhBP^{iPr}_3$)Fe(OCHO). A yellow THF solution (1 mL) of ($PhBP^{iPr}_3$)Fe(H)$_3$(PMe_3) (6.7 mg, 12 μmol) was degassed by freeze−pump−thaw cycles (3×). Subsequently, CO_2 (1 atm) was introduced to the thawed solution. The reaction was sealed and then stirred for 12 h at RT to give a light-yellow solution. The volatiles were removed to give an light-yellow solid. The material was triterated with pentane, and the solvent was removed in vacuo. The material was then redissolved in C_6H_6 (3 mL) and filtered through a glass frit to remove a black solid. Removal of the solvent in vacuo gave ($PhBP^{iPr}_3$)Fe(OCHO) (4.7 mg, 70%) as a light-yellow solid. Analytically pure material was obtained by layering HDMSO on top of a THF solution of ($PhBP^{iPr}_3$)Fe(OCHO) and allowing it to stand overnight. ^{1}H NMR (C_6D_6, 300 MHz): δ 41.1, 19.9, 18.6, 13.5, 9.2, 4.5, 3.6, 1.6, −1.2, −11.2, −12.1, −32.6, −37.7. μ_{eff} (C_6D_6, method of Evans, 20 °C): 5.0 μ_B (*S* = 2). IR (thin film, cm^{-1}): 1595 (m, ν_{asym}(O−C−O)), 1362 (m, ν_{sym}(O−C−O)). UV−vis (THF, nm {M^{-1} cm^{-1}}): 298 {1173}, 410 {274}. Anal. Calcd for $C_{28}H_{54}FeO_2P_3$: C, 57.75; H, 9.35. Found: C, 58.12; H, 9.67.

Synthesis of ($PhBP^{iPr}_3$)Fe(O^{13}CHO). The same procedures as those used to synthesize ($PhBP^{iPr}_3$)Fe(OCHO) were used here, except that $^{13}CO_2$ was used in place of CO_2. The ^{1}H NMR spectrum of ($PhBP^{iPr}_3$)Fe(O^{13}CHO) was identical with that of ($PhBP^{iPr}_3$)Fe(OCHO). IR (thin film, cm^{-1}): 1546 (m, ν_{asym}(O−^{13}C−O)), 1355 (m, ν_{sym}(O−^{13}C−O)).

Synthesis of [(NP^{iPr}_3)Fe(OCHO)](PF_6). A yellow THF solution (10 mL) of [(NP^{iPr}_3)Fe(N_2)(H)](PF_6) (29 mg, 40 μmol) was degassed by freeze−pump−thaw cycles (3×). Subsequently, CO_2 (1 atm) was introduced. The reaction was then sealed and stirred for 3 h at RT to give a colorless solution. The solvent was removed in vacuo to give a colorless solid. The material was triturated with pentane, and the solvent was removed in vacuo. The solid was washed with diethyl ether (3 × 1 mL) to give [(NP^{iPr}_3)Fe(OCHO)](PF_6) (29 mg, 97%) as a white solid. Analytically pure material was obtained by layering Et_2O on top of a THF solution of [(NP^{iPr}_3)Fe(OCHO)](PF_6) and allowing it to stand overnight at −35 °C. ^{1}H NMR (3:2 mixture of C_6D_6/THF-d_8, 300 MHz): δ 27.6, 9.4, 8.9, 6.4, 2.1, 1.9, 0.4, −8.3. ^{31}P NMR (3:2 mixture of C_6D_6/THF-d_8, 121 MHz): δ −144.4 (h, $^1J_{P-F}$ = 708 Hz, PF_6). ^{19}F NMR (3:2 mixture of C_6D_6/THF-d_8, 282 MHz): −73.4 (d, $^1J_{P-F}$ = 710 Hz, PF_6). μ_{eff} (C_6D_6, method of Evans, 20 °C): 5.1 μ_B (*S* = 2). IR (thin film, cm^{-1}): 1613 (m, ν_{asym}(O−C−O)). UV−vis (THF, nm {M^{-1} cm^{-1}}): 311 {shoulder, 660}, 379 {shoulder, 249}. Anal. Calcd for $C_{25}H_{55}F_6FeNO_2P_4$: C, 43.18; H, 7.97; N, 2.01. Found: C, 44.10; H, 8.25; N, 1.86.

Synthesis of [(NP^{iPr}_3)Fe(O^{13}CHO)](PF_6). The same procedures as those used to synthesize [(NP^{iPr}_3)Fe(OCHO)](PF_6) were used here, except that $^{13}CO_2$ was used in place of CO_2. The ^{1}H NMR spectrum of [(NP^{iPr}_3)Fe(O^{13}CHO)](PF_6) was identical with that of [(NP^{iPr}_3)Fe(OCHO)](PF_6). IR (thin film, cm^{-1}): 1579 (m, ν_{asym}(O−^{13}C−O)).

Synthesis of (TPB)FeCl. The procedures used to synthesize (TPB)FeBr[58] were used to synthesize (TPB)FeCl, except that $FeCl_2$ was used in place of $FeBr_2$. A Schlenk tube was charged with TPB (117 mg, 172 μmol), $FeCl_2$ (26 mg, 200 μmol), iron powder (113 mg, 2000 μmol), and THF (20 mL). The reaction was heated to 90 °C for 3 days with vigorous stirring, resulting in a color change of the liquid phase from light yellow to dark green-brown. The remaining iron powder was removed by filtration, and the solvent was removed in vacuo. The residue was taken up in toluene (5 mL), and the solvent was removed in vacuo. Pentane (200 mL) was added, and the mixture was stirred for 3 h and filtered. Removal of the solvent in vacuo yielded a yellow-brown powder of (TPB)FeCl (123 mg, 91%). ^{1}H NMR (C_6D_6, 300 MHz): δ 97.6, 35.1, 23.6, 9.6, 5.8, 3.4, 1.9, −0.2, −2.3, −22.5. μ_{eff} (C_6D_6, method of Evans, 20 °C): 4.1 μ_B (*S* = 2). UV−vis (THF, nm {M^{-1} cm^{-1}}): 275 {14086}, 317 {10385}, 556 {sh, 80}, 774 {66}, 897 {91}. Anal. Calcd for $C_{36}H_{54}BClFeP_3$: C, 63.41; H, 7.98. Found: C, 64.06; H, 8.89.

Synthesis of (TPB)Fe(OCHO). A yellow benzene solution (6 mL) of (TPB)(μ-H)Fe(N_2)(H) (20.7 mg, 31 μmol) was degassed by freeze−pump−thaw cycles (3×). Subsequently, CO_2 (1 atm) was introduced. The reaction was then sealed, and the yellow solution was mixed for 1 h at RT. The solvent was lyophilized in vacuo to give (TPB)Fe(OCHO) as a dark-yellow solid (21.0 mg, 99%). Analytically pure material was obtained by cooling a concentrated pentane solution of (TPB)Fe(OCHO) to −35 °C overnight. ^{1}H NMR (C_6D_6, 300 MHz): δ 86.1, 66.3, 38.5, 26.3, 15.5, 4.3, 2.7, 1.4, 1.0, −0.7, −2.6, −3.5, −24.1. μ_{eff} (C_6D_6, method of Evans, 20 °C): 4.2 μ_B (*S* = 2). IR (thin film, cm^{-1}): 1627 (m, ν_{asym}(O−C−O)), 1291 (m, ν_{sym}(O−C−O)). UV−vis (THF, nm {M^{-1} cm^{-1}}): 278 {16400}, 317 {12800}, 773 {br abs, 98}, 958 {127}. Anal. Calcd for $C_{37}H_{55}BFeO_2P_3$: C, 64.27; H, 8.02. Found: C, 63.16; H, 7.75.

Synthesis of (TPB)Fe(O^{13}CHO). The same procedures as those used to synthesize (TPB)Fe(OCHO) were used, except that $^{13}CO_2$ was used in place of CO_2. The ^{1}H NMR spectrum was identical with that of (TPB)Fe(OCHO). IR (thin film, cm^{-1}): 1588 (m, ν_{asym}(O−^{13}C−O)), 1269 (m, ν_{sym}(O−^{13}C−O)).

Reaction of (TPB)Fe(N_2) with Formic Acid. (TPB)Fe(N_2) (8.2 mg, 12.1 μmol) in 2 mL of THF was charged into a round-bottomed flask, and the flask was sealed with a rubber septum. Formic acid (3 μL, 80.3 μmol) was added by syringe through the septum, immediately resulting in effervescence of H_2 and a yellow-brown solution. The solution was allowed to stir for a few minutes before the volatiles were removed in vacuo to reveal a brown solid. The material was redissolved in benzene and filtered. Removal of the volatiles in vacuo revealed a brown powder of (TPB)Fe(OCHO) (8.1 mg, 96%).

DOI: 10.1021/ic502508p
Inorg. Chem. 2015, 54, 5124−5135

NMR and IR spectral data for this material were identical with those of (TPB)Fe(OCHO).

Deprotonation of [(SiP$^{iPr}_3$)Fe(H$_2$)](BAr$^F_4$) with Et$_3$N. [(SiP$^{iPr}_3$)Fe(N$_2$)](BAr$^F_4$) (14.6 mg, 9.4 μmol) and triethylamine (1.7 μL, 9.7 μmol) were charged into an NMR tube with a *J*-young valve with C_6D_6 and THF-d_8 (ca. 0.4 and 0.1 mL, respectively), yielding a green solution. The solution was degassed by freeze−pump−thaw cycles (3×), revealing an orange solution consistent with [(SiP$^{iPr}_3$)Fe(THF)](BAr$^F_4$). H_2 (1 atm) was charged into the reaction mixture, yielding a transient gray solution (consistent with [(SiP$^{iPr}_3$)Fe(H$_2$)](BAr$^F_4$) that immediately changed to orange-yellow upon mixing. The reaction was mixed overnight. The NMR data of the iron species in this reaction mixture were identical with those of (SiP$^{iPr}_3$)Fe(H$_2$)(H).[43] The volatiles were removed in vacuo, and the resulting yellow solid was extracted with pentane. The pentane was removed in vacuo to yield a yellow solid of (SiP$^{iPr}_3$)Fe(N$_2$)(H) (5.1 mg, 88%). The ^{1}H and ^{31}P NMR spectra of this material are identical with those of (SiP$^{iPr}_3$)Fe(N$_2$)(H).

Quantifying H_2 Loss from the Reaction of (TPB)(μ-H)Fe(N$_2$)(H) with CO_2. Procedures similar to those of the synthesis of (TPB)Fe(OCHO) were followed. (TPB)(μ-H)Fe(N$_2$)(H) (20.0 mg, 31 μmol) was dissolved in 6 mL of benzene and charged into a calibrated 200 mL Schlenk tube having a Teflon valve and a 24/40 side joint. The solution was degassed by freeze−pump−thaw cycles (3×), opened to CO_2 (1 atm) and agitated for ca. 5 s to ensure adequate dissolution of CO_2. The reaction was then sealed at the Teflon valve joint and also with a rubber septum at the 24/40 joint. The reaction was stirred vigorously for 30 min, the Teflon valve was opened, and the headspace was sampled through the rubber septum with a 10 mL gastight syringe, being careful to ensure adequate mixing of the gases from the reaction headspace into the 24/40 joint's headspace by repeated extraction and reinjection (3×) of the headspace gas with the gastight syringe before a final aliquot was taken for analysis by GC-TCD. A total of 0.44 equiv of H_2 [relative to (TPB)(μ-H)Fe(N$_2$)(H)] was found.

Quantifying H_2 Loss from the Reaction of (TPB)Fe(N$_2$) with Formic Acid. Procedures similar to those of the synthesis of (TPB)Fe(OCHO) from formic acid and (TPB)Fe(N$_2$) were followed. (TPB)Fe(N$_2$) (24.5 mg, 36 μmol) in benzene (3 mL) was charged into a calibrated 100 mL round-bottomed flask and sealed with a rubber septum. Formic acid (1.3 μL, 36 μmol) was added by syringe. Effervescence was immediately visible. The reaction was allowed to stir for a few minutes before the headspace was sampled through the rubber septum with a 10 mL gastight syringe for analysis by GC-TCD. A total of 0.42 equiv of H_2 [relative to (TPB)Fe(N$_2$)] was found.

Metathesis Reactions of Iron Formate Complexes with (Et$_3$NH)Cl. (Et$_3$NH)Cl (10 equiv) was charged into a methanol or benzene solution of (SiP$^{iPr}_3$)Fe(OCHO), (SiP$^{Ph}_3$)Fe(OCHO), (PhBP$^{iPr}_3$)Fe(OCHO), [(NP$^{iPr}_3$)Fe(OCHO)](PF$_6$), or (TPB)Fe(OCHO). The resulting suspension was stirred overnight and then filtered through a glass frit. The filtrate was concentrated in vacuo into a solid and then extracted. For (SiP$^{iPr}_3$)Fe(OCHO), (SiP$^{Ph}_3$)Fe(OCHO), (PhBP$^{iPr}_3$)Fe(OCHO), and (TPB)Fe(OCHO), pentane (3 × 1 mL) was used for extraction, while a 4:1 C_6H_6/THF mixture (3 × 1 mL) was used for [(NP$^{iPr}_3$)Fe(OCHO)](PF$_6$)). The respective ^{1}H NMR and IR spectra of the extract showed conversion to (SiP$^{iPr}_3$)FeCl, (SiP$^{Ph}_3$)FeCl, (PhBP$^{iPr}_3$)FeCl, [(NP$^{iPr}_3$)FeCl](PF$_6$), or (TPB)FeCl.

CO_2 Hydrogenation Catalysis Protocols. High-pressure hydrogenation reactions were run in a Parr Instruments Company 4590 Micro Bench Top Reactor, with a 20 mL reaction vessel, controlled by a Parr Instruments Company 4834 controller. In a typical catalytic run, an iron precatalyst in 0.1 mL of THF (to solubilize iron precatalyst), 10 mL of methanol, and 1 mL of triethylamine were charged into the Parr reactor. The reactor was sealed, stirred with the attached mechanical stirrer (100 rpm), and charged with CO_2 until the desired pressure at equilibrium was achieved (ca. 10 min). H_2 was subsequently added into the reactor. The gas inlet port was closed, and the reactor was then heated at 100 °C for 20 h. Changes to these conditions were made as described in Tables 2−4 and S1 in the SI. At the conclusion of the reaction, the reactor was cooled to 10 °C with an ice bath over ca. 1.5 h, and the pressure was slowly released through a needle valve. An aliquot of the crude solution was immediately taken for methylformate quantification by GC-FID. The aliquot was then recombined with the crude solution, DMF was added (1 mmol), and 25 μL of this solution was taken into 0.5 mL of CD_2Cl_2 for triethylammonium formate quantification by ^{1}H NMR spectroscopy.

Similar procedures were followed for the low-pressure reactions (1 atm of CO_2 and 1−4 atm of H_2), where the reactions were run in a 15 mL Schlenk tube that has a Teflon valve. The solution was degassed by freeze−pump−thaw cycles (3×), and CO_2 (1 atm) was introduced into the vessel at RT. For the reactions requiring 4 atm of H_2, the entire body of the Schlenk tube was then cooled in a liquid-N_2 bath and 1 atm (RT) of H_2 was introduced. For reactions requiring 1 atm of H_2, the Schlenk tube was cooled with liquid N_2 up to the solution level only and 1 atm (RT) of H_2 was introduced.

Analysis of the Iron Content Postcatalytic Reaction. The reaction was worked up similarly to the procedures described above for the hydrogenation runs. After the reactor was depressurized, it was brought into the glovebox for workup. The crude solution was transferred to a scintillation vial, and the volatiles were removed in vacuo. The resulting light-yellow solid was dissolved in C_6D_6 and analyzed by ^{1}H and ^{31}P NMR spectroscopy.

Hydricity Determination. The hydricity was experimentally determined using the method presented by DuBois et al.[52,53] The equilibrium of eq 3 (Scheme 1) with a given base (proton sponge, 2,6-lutidine, or 2,4,6-trimethylpyridine) was measured in THF-d_8. With proton sponge as the base, [(SiP$^{iPr}_3$)Fe(N$_2$)](BAr$^F_4$) (8.0 mg, 5.1 μmol) was mixed with proton sponge (1.1 mg, 5.1 μmol) and the integration standard 1,3,5-trimethoxybenzene (1.2 mg, 7.1 μmol) in THF-d_8 (0.5 mL). With 2,6-lutidine as the base, [(SiP$^{iPr}_3$)Fe(N$_2$)](BAr$^F_4$) (8.7 mg, 5.6 μmol) was mixed with 2,6-lutidine (34 μL, 292 μmol) and the integration standard 1,3,5-trimethoxybenzene (1.1 mg, 6.5 μmol) in THF-d_8 (0.5 mL). With 2,4,6-trimethylpyridine as the base, [(SiP$^{iPr}_3$)Fe(N$_2$)](BAr$^F_4$) (8.3 mg, 5.3 μmol) was mixed with 2,4,6-trimethylpyridine (1.6 μL, 19.8 μmol) and the integration standard 1,3,5-trimethoxybenzene (1.3 mg, 7.7 μmol) with THF-d_8 (0.5 mL). The solutions were degassed by freeze−pump−thaw cycles (3×), and H_2 (1 atm) was introduced. The solutions were mixed using a mechanical rotator at a rate of ca. 12 min^{-1}, and the reaction was monitored by ^{1}H NMR spectroscopy until equilibration: proton sponge, 6 days; 2,6-lutidine, 5 days; 2,4,6-trimethylpyridine, 5 days. Equation 3−5 were used to calculate ΔG_{H^-}. The equilibrium between [(SiP$^{iPr}_3$)Fe(H$_2$)](BAr$^F_4$) and its THF adduct [(SiP$^{iPr}_3$)Fe(H$_2$)](BAr$^F_4$) was also taken into account in the calculations (see the SI).

UV−Vis Titration. The UV−vis titration experiments of [(SiP$^{iPr}_3$)Fe(N$_2$)](BAr$^F_4$) (4.8 mM) with Li(OCHO) (48 mM) in THF was performed by adding aliquots of the formate solution to a solution of the iron complex. The decay of [(SiP$^{iPr}_3$)Fe(N$_2$)](BAr$^F_4$) was monitored, with the absorbance at 752 nm used for fitting to a quadratic equation against K_{eq}. After the addition of 1 equiv of Li(OCHO), a spectrum corresponding to (SiP$^{iPr}_3$)Fe(OCHO) was observed.

■ ASSOCIATED CONTENT

Supporting Information

NMR, IR, and UV−vis spectra, along with detailed catalytic hydrogenation results and a detailed description of the hydricity calculations. This material is available free of charge via the Internet at http://pubs.acs.org.

■ AUTHOR INFORMATION

Corresponding Author

*E-mail: jpeters@caltech.edu.

Notes

The authors declare no competing financial interest.

DOI: 10.1021/ic502508p
Inorg. Chem. 2015, 54, 5124−5135

■ ACKNOWLEDGMENTS

This material is based upon work performed by the Joint Center of Artificial Photosynthesis, a DOE Energy Innovation Hub, supported through the Office of Science of the U.S. Department of Energy under Award DE-SC0004993. The Bercaw Group at the California Institute of Technology is acknowledged for their assistance with the high-pressure reactions. GC-FID instrumentation at the Environmental Analysis Center (EAC) at the California Institute of Technology was used in this work. We acknowledge Dr. Nathan Dalleska of the EAC for his assistance with the GC-FID measurements.

■ REFERENCES

(1) *Carbon Dioxide as Chemical Feedstock*; Wiley-VCH Verlag GmbH & Co. KGaA: Weinheim, Germany, 2010.
(2) Olah, G. A. *Angew. Chem., Int. Ed.* **2013**, *52*, 104−107.
(3) Enthaler, S.; von Langermann, J.; Schmidt, T. *Energy Environ. Sci.* **2010**, *3*, 1207−1217.
(4) Arakawa, H.; Aresta, M.; Armor, J. N.; Barteau, M. A.; Beckman, E. J.; Bell, A. T.; Bercaw, J. E.; Creutz, C.; Dinjus, E.; Dixon, D. A.; Domen, K.; DuBois, D. L.; Eckert, J.; Fujita, E.; Gibson, D. H.; Goddard, W. A.; Goodman, D. W.; Keller, J.; Kubas, G. J.; Kung, H. H.; Lyons, J. E.; Manzer, L. E.; Marks, T. J.; Morokuma, K.; Nicholas, K. M.; Periana, R.; Que, L.; Rostrup-Nielson, J.; Sachtler, W. M. H.; Schmidt, L. D.; Sen, A.; Somorjai, G. A.; Stair, P. C.; Stults, B. R.; Tumas, W. *Chem. Rev.* **2001**, *101*, 953−996.
(5) Appel, A. M.; Bercaw, J. E.; Bocarsly, A. B.; Dobbek, H.; DuBois, D. L.; Dupuis, M.; Ferry, J. G.; Fujita, E.; Hille, R.; Kenis, P. J. A.; Kerfeld, C. A.; Morris, R. H.; Peden, C. H. F.; Portis, A. R.; Ragsdale, S. W.; Rauchfuss, T. B.; Reek, J. N. H.; Seefeldt, L. C.; Thauer, R. K.; Waldrop, G. L. *Chem. Rev.* **2013**, *113*, 6621−6658.
(6) Benson, E. E.; Kubiak, C. P.; Sathrum, A. J.; Smieja, J. M. *Chem. Soc. Rev.* **2009**, *38*, 89−99.
(7) Cokoja, M.; Bruckmeier, C.; Rieger, B.; Herrmann, W. A.; Kühn, F. E. *Angew. Chem., Int. Ed.* **2011**, *50*, 8510−8537.
(8) *The Handbook of Homogeneous Hydrogenation*; Wiley-VCH Verlag GmbH: Weinheim, Germany, 2008.
(9) Jessop, P. G.; Ikariya, T.; Noyori, R. *Nature* **1994**, *368*, 231−233.
(10) Tanaka, R.; Yamashita, M.; Nozaki, K. *J. Am. Chem. Soc.* **2009**, *131*, 14168−14169.
(11) Graf, E.; Leitner, W. *J. Chem. Soc., Chem. Commun.* **1992**, 623−624.
(12) Lau, C. P.; Chen, Y. Z. *J. Mol. Catal. A: Chem.* **1995**, *101*, 33−36.
(13) Erlandsson, M.; Landaeta, V. R.; Gonsalvi, L.; Peruzzini, M.; Phillips, A. D.; Dyson, P. J.; Laurenczy, G. *Eur. J. Inorg. Chem.* **2008**, *2008*, 620−627.
(14) Huff, C. A.; Sanford, M. S. *J. Am. Chem. Soc.* **2011**, *133*, 18122−18125.
(15) Huff, C. A.; Sanford, M. S. *ACS Catal.* **2013**, 2412−2416.
(16) Schaub, T.; Paciello, R. A. *Angew. Chem., Int. Ed.* **2011**, *50*, 7278−7282.
(17) Wang, W.-H.; Muckerman, J. T.; Fujita, E.; Himeda, Y. *ACS Catal.* **2013**, *3*, 856−860.
(18) Langer, R.; Diskin-Posner, Y.; Leitus, G.; Shimon, L. J. W.; Ben-David, Y.; Milstein, D. *Angew. Chem., Int. Ed.* **2011**, *50*, 9948−9952.
(19) Federsel, C.; Boddien, A.; Jackstell, R.; Jennerjahn, R.; Dyson, P. J.; Scopelliti, R.; Laurenczy, G.; Beller, M. *Angew. Chem., Int. Ed.* **2010**, *49*, 9777−9780.
(20) Ziebart, C.; Federsel, C.; Anbarasan, P.; Jackstell, R.; Baumann, W.; Spannenberg, A.; Beller, M. *J. Am. Chem. Soc.* **2012**, *134*, 20701−20704.
(21) Evans, G. O.; Newell, C. J. *Inorg. Chim. Acta* **1978**, *31*, L387−L389.
(22) Tai, C.-C.; Chang, T.; Roller, B.; Jessop, P. G. *Inorg. Chem.* **2003**, *42*, 7340−7341.
(23) Inoue, Y.; Sasaki, Y.; Hashimoto, H. *J. Chem. Soc., Chem. Commun.* **1975**, 718−719.
(24) Haynes, P.; Slaugh, L. H.; Kohnle, J. F. *Tetrahedron Lett.* **1970**, *11*, 365−368.
(25) Federsel, C.; Ziebart, C.; Jackstell, R.; Baumann, W.; Beller, M. *Chem.—Eur. J.* **2012**, *18*, 72−75.
(26) Jeletic, M. S.; Mock, M. T.; Appel, A. M.; Linehan, J. C. *J. Am. Chem. Soc.* **2013**, *135*, 11533−11536.
(27) Kumar, N.; Camaioni, D.; Dupuis, M.; Raugei, S.; Appel, A. M. *Dalton Trans.* **2014**, *43*, 11803−11106.
(28) Badiei, Y. M.; Wang, W.-H.; Hull, J. F.; Szalda, D. J.; Muckerman, J. T.; Himeda, Y.; Fujita, E. *Inorg. Chem.* **2013**, *52*, 12576−12586.
(29) Field, L. D.; Lawrenz, E. T.; Shaw, W. J.; Turner, P. *Inorg. Chem.* **2000**, *39*, 5632−5638.
(30) Allen, O. R.; Dalgarno, S. J.; Field, L. D. *Organometallics* **2008**, *27*, 3328−3330.
(31) Field, L. D.; Shaw, W. J.; Turner, P. *Chem. Commun.* **2002**, 46−47.
(32) Hills, A.; Hughes, D. L.; Jimenez-Tenorio, M.; Leigh, G. J. *J. Organomet. Chem.* **1990**, *391*, C41−C44.
(33) Bianco, V. D.; Doronzo, S.; Gallo, N. *Inorg. Nucl. Chem. Lett.* **1980**, *16*, 97−99.
(34) Bianco, V. D.; Doronzo, S.; Rossi, M. *J. Organomet. Chem.* **1972**, *35*, 337−339.
(35) Estes, D. P.; Vannucci, A. K.; Hall, A. R.; Lichtenberger, D. L.; Norton, J. R. *Organometallics* **2011**, *30*, 3444−3447.
(36) DuBois, D. L.; Berning, D. E. *Appl. Organomet. Chem.* **2000**, *14*, 860−862.
(37) Lee, Y.; Mankad, N. P.; Peters, J. C. *Nat. Chem.* **2010**, *2*, 558−565.
(38) Betley, T. A.; Peters, J. C. *J. Am. Chem. Soc.* **2003**, *125*, 10782−10783.
(39) Betley, T. A.; Peters, J. C. *J. Am. Chem. Soc.* **2004**, *126*, 6252−6254.
(40) Anderson, J. S.; Rittle, J.; Peters, J. C. *Nature* **2013**, *501*, 84−87.
(41) Anderson, J. S.; Moret, M.-E.; Peters, J. C. *J. Am. Chem. Soc.* **2012**, *135*, 534−537.
(42) Creutz, S. E.; Peters, J. C. *J. Am. Chem. Soc.* **2013**, *136*, 1105−1115.
(43) Lee, Y.; Kinney, R. A.; Hoffman, B. M.; Peters, J. C. *J. Am. Chem. Soc.* **2011**, *133*, 16366−16369.
(44) Fong, H.; Moret, M.-E.; Lee, Y.; Peters, J. C. *Organometallics* **2013**, *32*, 3053−3062.
(45) Daida, E. J.; Peters, J. C. *Inorg. Chem.* **2004**, *43*, 7474−7485.
(46) MacBeth, C. E.; Harkins, S. B.; Peters, J. C. *Can. J. Chem.* **2005**, *83*, 332−340.
(47) Rittle, J.; Peters, J. C. *Proc. Natl. Acad. Sci. U. S. A.* **2013**, *110*, 15898−15903.
(48) Heinekey, D. M.; van Roon, M. *J. Am. Chem. Soc.* **1996**, *118*, 12134−12140.
(49) THF is known to bind competitively with H_2 on $[(SiP^{iPr}_3)Fe(L)](BAr^F_4]$ (where L = THF or H_2), and the THF/H_2 binding equilibrium was taken into account in the calculations; see the SI.
(50) The pK_a of $[(SiP^{iPr}_3)Fe(H_2)](BAr^F_4)$ was estimated using the Morris method. These calculations rely on the ligand acidity constants for each of the ligands of the conjugate base metal complex, which in this case is the deprotonation product $(SiP^{iPr}_3)Fe(H_2)(H)$. We note that the ligand acidity constants for H_2 and the formally Si^- ligands of the conjugate base complex are not known. We therefore used the reported ligand acidity constants of C_2H_4 as a model for the H_2 ligand and of CH_3^-/H^- as a model for the Si^- ligand unit for these calculations. See ref 51.
(51) Morris, R. H. *J. Am. Chem. Soc.* **2014**, *136*, 1948−1959.
(52) Ciancanelli, R.; Noll, B. C.; DuBois, D. L.; DuBois, M. R. *J. Am. Chem. Soc.* **2002**, *124*, 2984−2992.
(53) Price, A. J.; Ciancanelli, R.; Noll, B. C.; Curtis, C. J.; DuBois, D. L.; DuBois, M. R. *Organometallics* **2002**, *21*, 4833−4839.

DOI: 10.1021/ic502508p
Inorg. Chem. 2015, 54, 5124−5135

(54) Abdur-Rashid, K.; Fong, T. P.; Greaves, B.; Gusev, D. G.; Hinman, J. G.; Landau, S. E.; Lough, A. J.; Morris, R. H. *J. Am. Chem. Soc.* **2000**, *122*, 9155−9171.
(55) Chen, J. Z.; Szalda, D. J.; Fujita, E.; Creutz, C. *Inorg. Chem.* **2010**, *49*, 9380−9391.
(56) Gibson, D. H. *Coord. Chem. Rev.* **1999**, *185*−*186*, 335−355.
(57) Whited, M. T.; Mankad, N. P.; Lee, Y.; Oblad, P. F.; Peters, J. C. *Inorg. Chem.* **2009**, *48*, 2507−2517.
(58) Moret, M.-E.; Peters, J. C. *Angew. Chem., Int. Ed.* **2011**, *50*, 2063−2067.
(59) The $\{M-B\}^n$ notation refers to the number of valence electrons that are formally assigned to the metal (e.g., iron) and shared with the boron atom. For a discussion of M−B bonding, see: (a) Hill, A. F. *Organometallics* **2006**, *25*, 4741−4743. (b) Parkin, G. *Organometallics* **2006**, *25*, 4744−4747.
(60) Marks, T. J.; Kolb, J. R. *Chem. Rev.* **1977**, *77*, 263−293.
(61) Munshi, P.; Main, A. D.; Linehan, J. C.; Tai, C.-C.; Jessop, P. G. *J. Am. Chem. Soc.* **2002**, *124*, 7963−7971.
(62) Wesselbaum, S.; vom Stein, T.; Klankermayer, J.; Leitner, W. *Angew. Chem., Int. Ed.* **2012**, *51*, 7499−7502.
(63) Mellone, I.; Peruzzini, M.; Rosi, L.; Mellmann, D.; Junge, H.; Beller, M.; Gonsalvi, L. *Dalton Trans.* **2013**, *42*, 2495−2501.
(64) Saouma, C. T.; Lu, C. C.; Day, M. W.; Peters, J. C. *Chem. Sci.* **2013**, *4*, 4042−4051.
(65) Gambarotta, S.; Arena, F.; Floriani, C.; Zanazzi, P. F. *J. Am. Chem. Soc.* **1982**, *104*, 5082−5092.
(66) Bielinski, E. A.; Lagaditis, P. O.; Zhang, Y.; Mercado, B. Q.; Würtele, C.; Bernskoetter, W. H.; Hazari, N.; Schneider, S. *J. Am. Chem. Soc.* **2014**, *136*, 10234−10237.
(67) Drake, J. L.; Manna, C. M.; Byers, J. A. *Organometallics* **2013**, *32*, 6891−6894.
(68) Otera, J.; Nishikido, J. *Esterification*; Wiley-VCH Verlag GmbH & Co. KGaA: Weinheim, Germany, 2010.
(69) Kaljurand, I.; Kütt, A.; Sooväli, L.; Rodima, T.; Mäemets, V.; Leito, I.; Koppel, I. A. *J. Org. Chem.* **2005**, *70*, 1019−1028.
(70) Matsubara, Y.; Fujita, E.; Doherty, M. D.; Muckerman, J. T.; Creutz, C. *J. Am. Chem. Soc.* **2012**, *134*, 15743−15757.
(71) Brunner, E. *J. Chem. Eng. Data* **1985**, *30*, 269−273.

DOI: 10.1021/ic502508p
Inorg. Chem. 2015, 54, 5124−5135